DOI: 10.1534/genetics.109.108571

The Developmentally Active and Stress-Inducible Noncoding *hsrω* Gene Is a Novel Regulator of Apoptosis in Drosophila

Moushami Mallik and Subhash C. Lakhotia[1]

Cytogenetics Laboratory, Department of Zoology, Banaras Hindu University, Varanasi 221 005, India

Manuscript received August 12, 2009
Accepted for publication September 5, 2009

ABSTRACT

The large nucleus limited noncoding hsrω-n RNA of *Drosophila melanogaster* is known to associate with a variety of heterogeneous nuclear RNA-binding proteins (hnRNPs) and certain other RNA-binding proteins to assemble the nucleoplasmic omega speckles. In this article, we show that RNAi-mediated depletion of this noncoding RNA dominantly suppresses apoptosis, in eye and other imaginal discs, triggered by induced expression of Rpr, Grim, or caspases (initiator as well as effector), all of which are key regulators/effectors of the canonical caspase-mediated cell death pathway. We also show, for the first time, a genetic interaction between the noncoding hsrω transcripts and the c-Jun N-terminal kinase (JNK) signaling pathway since downregulation of hsrω transcripts suppressed JNK activation. In addition, *hsrω-RNAi* also augmented the levels of Drosophila Inhibitor of Apoptosis Protein 1 (DIAP1) when apoptosis was activated. Suppression of induced cell death following depletion of hsrω transcripts was abrogated when the *DIAP1-RNAi* transgene was coexpressed. Our results suggest that the hsrω transcripts regulate cellular levels of DIAP1 via the hnRNP Hrb57A, which physically interacts with DIAP1, and any alteration in levels of the hsrω transcripts in eye disc cells enhances association between these two proteins. Our studies thus reveal a novel regulatory role of the hsrω noncoding RNA on the apoptotic cell death cascade through multiple paths. These observations add to the diversity of regulatory functions that the large noncoding RNAs carry out in the cells' life.

THE noncoding *hsrω* gene, located at the 93D4 cytogenetic region on the right arm of chromosome 3 of *Drosophila melanogaster*, produces several noncoding transcripts as the functional end products (reviewed in Lakhotia 2003). It is expressed in a developmentally regulated manner and is also inducible under conditions of stress like heat shock, amide treatment, and recovery from anoxia, etc. (Mutsuddi and Lakhotia 1995; Lakhotia 2003). Of the multiple noncoding transcripts produced by this locus, the nucleus limited hsrω-n transcript colocalizes with a variety of heterogeneous nuclear RNA-binding proteins (hnRNPs) to form fine nucleoplasmic omega speckles, which act as dynamic sinks to regulate the trafficking of hnRNPs and other related RNA-binding proteins (Lakhotia *et al.* 1999; Prasanth *et al.* 2000; Jolly and Lakhotia 2006). The hsrω transcripts play a crucial role in normal development and differentiation in the fly, since nullisomy for this gene leads to a high degree of embryonic lethality (Ray and Lakhotia 1998). All Drosophila species show a functional homolog of this gene (Lakhotia and Singh 1982; E. Mutt and S. C. Lakhotia, unpublished data). To understand physiological roles of the noncoding *hsrω* gene, we established *EP* and *RNAi* lines (Mallik and Lakhotia 2009) designed to, respectively, overexpress or deplete hsrω transcript levels using the UAS/GAL4 expression system (Brand and Perrimon 1993). Initial studies showed that RNAi-mediated eye-specific depletion of hsrω transcripts rescued the retinal damage seen in flies with two copies of the *GMR-GAL4* transgene. Furthermore, other studies in our laboratory demonstrated that misexpression of the hsrω transcripts modulates poly(Q)-induced neurodegeneration in fly models (Sengupta and Lakhotia 2006; Mallik and Lakhotia 2009). Since eye degeneration in *GMR-GAL4* homozygous individuals is due to an elevated incidence of apoptosis (Kramer and Staveley 2003) and since proteins with expanded poly(Q) also trigger apoptosis (Sanchez *et al.* 1999; Evert *et al.* 2000; Gunawardena *et al.* 2003), we undertook the present study to examine if the hsrω transcripts play a role in the cell death pathway(s).

Apoptosis is a highly conserved and the most common form of programmed cell death (PCD), which is essential for normal development of multicellular organisms. Apoptosis requires activation of a conserved class of cysteine proteases or caspases to effect de-

[1] *Corresponding author:* Cytogenetics Laboratory, Department of Zoology, Banaras Hindu University, Varanasi 221 005, India.
E-mail: lakhotia@bhu.ac.in

struction of the cell (Lee and Baehrecke 2001). Inactive apical or initiator caspases are proteolytically cleaved to produce effector caspases that eventually bring about cell death through breakdown of protein substrates. Seven caspases are known in Drosophila although all of them are not involved in apoptosis. These are grouped into two categories on the basis of the presence of a regulator prodomain. The three upstream or apical caspases, Dronc, Dream, and Dredd, have long prodomains. The effector or downstream caspases, DrICE, Dcp-1, Decay, and Damm, have short prodomains and are the direct mediators of apoptosis (Riedl and Shi 2004; Hay and Guo 2006). In Drosophila, Drosophila Inhibitor of Apoptosis Protein 1 (DIAP1) keeps the initiator and effector caspases inactive by binding with them and thus acts as the focal point for regulation of apoptosis (Arya *et al.* 2007). DIAP1 directly inhibits processing of the initiator caspases so that DIAP1/thread mutants exhibit excessive apoptosis because of the unchecked processing and activation of Dronc, Dcp-1, and DrICE (Hawkins *et al.* 1999; Meier *et al.* 2000; Yoo *et al.* 2002; Chai *et al.* 2003; Yan *et al.* 2004). Caspase-mediated cell death in Drosophila is activated by several small proteins like Reaper (Rpr), Head involution defective (Hid), and Grim, collectively known as the RHG proteins; their N terminus binds to DIAP1, resulting in depletion of its activity so that the apical and effector caspases become active and trigger apoptosis (Wang *et al.* 1999; Wu *et al.* 2001; Yoo *et al.* 2002).

In the present study, we investigated interaction(s) of the noncoding hsrω transcripts with a number of candidate regulators of the canonical apoptotic cascade. We used GAL4-driven expression of the *hsrω-RNAi* transgenes (Mallik and Lakhotia 2009) or of the overexpressing *EP3037* and *EP93D* alleles of *hsrω* (Sengupta and Lakhotia 2006; Mallik and Lakhotia 2009) to examine effects of altered levels of the hsrω transcripts on apoptotic cell death brought about by coexpression of the various transgenes that induce or inhibit apoptosis. Our results show that while depletion of hsrω transcripts through conditional RNAi blocked caspase-mediated induced apoptosis, overexpression significantly enhanced the cell death phenotypes. We show, for the first time, that the noncoding hsrω transcripts regulate DIAP1 levels via the Hrb57A hnRNP, since depletion as well as overexpression of hsrω transcripts enhanced the association between Hrb57A and DIAP1. Consequences of the enhanced association of Hrb57A and DIAP1 seem to depend upon the levels of hsrω transcripts since when depleted, the DIAP1 remained active while in cells with elevated hsrω transcripts, DIAP1, although present, failed to block caspase activity. We further show that the hsrω transcripts are necessary for activation of c-Jun N-terminal kinase (JNK)-mediated apoptosis in Drosophila.

MATERIALS AND METHODS

Fly genetics: Fly cultures were maintained at 23° ± 1° on standard food containing agar, maize powder, yeast, and sugar; the desired fly crosses were made following standard procedures. Oregon R^+ was used as the wild-type strain. The following transgenic lines were used:

y w; +/+; GMR-rpr/TM6 (White *et al.* 1996)
y w^{67c23}*; GMR-hid/CyO; +/+* (Grether *et al.* 1995)
y w; +/+; GMR-grim/TM6B (Hawkins *et al.* 2000)
w; +/+; UAS-pro-dronc^{W}*/TM3, Ser* (Meier *et al.* 2000)
w; +/+; UAS-pro-dronc^{S}*/TM3, Ser* (Meier *et al.* 2000)
w; +/+; UAS-ΔN dronc/TM3, Ser (Meier *et al.* 2000)
y w; +/+; GMR-ΔN-dcp-1/GMR-ΔN-dcp-1 (Song *et al.* 2000)
w; GMR-GAL4 UAS-DIAP1-RNAi/CyO; +/+ (Leulier *et al.* 2006)
w^{1118}*; UAS-egr/CyO; +/+* (Igaki *et al.* 2002)
w^{1118}*; UAS-dTAK1/UAS-dTAK1; +/+* (Takatsu *et al.* 2000)
w; EP0578 (DTRAF1)/EP0578 (DTRAF1); +/+ (Cha *et al.* 2003)
w^{+}*; +/+; puc[E69]/TM3,* Sb^{1} (Ring and Martinez Arias 1993)
w; +/+; UAS-DIAP1/UAS-DIAP1* (Bloomington Stock Center, Bloomington, IN)
w^{1118}*; GMR-GAL4/GMR-GAL4; +/+* (Hay *et al.* 1994)
y w^{1118}*; +/+; vg-GAL4/vg-GAL4* (Bloomington Stock Center)
y^{1} *w*; Act5C-GAL4/CyO,* y^{+}*; +/+* (Bloomington Stock Center)
w^{1118}*; UAS-rpr/UAS-rpr; +/+* (Bloomington Stock Center)
w^{1118}*; GMR-argos/GMR-argos* (Sawamoto *et al.* 1998)
w; GMR-GAL4 UAS-ΔN DER/CyO; +/+ (Freeman 1996)
w/w; UAS-hsrω-RNAi^{2}*/UAS-hsrω-RNAi*^{2}*; +/+* (Mallik and Lakhotia 2009)
w/w; +/+; UAS-hsrω-RNAi^{3}*/UAS-hsrω-RNAi*^{3} (Mallik and Lakhotia 2009)
w/w; UAS-hsrω-RNAi(2X)/UAS-hsrω-RNAi(2X); +/+ (generated in our laboratory)
w/w; +/+; EP93D/EP93D (Akanksha *et al.* 2008)
w/w; +/+; EP3037/EP3037 (Mallik and Lakhotia 2009).

Of the three *hsrω-RNAi* transgenic lines available with us, the *hsrω-RNAi*^{3} transgenic line was used, unless otherwise mentioned, in most of the present studies. The *hsrω-RNAi* transgene from the desired transgenic line or the *EP93D* or *EP3037* alleles (Mallik and Lakhotia 2009) were introgressed or recombined, as required, with the *GMR-GAL4* driver and used in various crosses to generate the desired genotypes. Most of the genetic interactions were carried out with single copies of *hsrω-RNAi*, *EP93D*, or *EP3037*, unless stated otherwise.

Examination of eye structure: Flies of the desired genotype were etherized and the external morphology of their eyes was examined at 40× magnification under a LEICA MS5 stereobinocular microscope. The number of flies examined in each case is stated in RESULTS. Eyes were photographed using a Sony Digital Camera (DSC-75) attached to a Zeiss Stemi SV6 stereobinocular microscope.

Nail polish imprints of eye surfaces from 1- to 2-day-old adult flies were prepared as described earlier (Arya and Lakhotia 2006). Nail polish imprints of eyes of 5–10 flies of each genotype were examined under a Nikon E800 microscope, using a 20× objective with DIC optics.

The arrangement of photoreceptor rhabdomeres in adult eyes (wild type or those expressing various transgenes/mutants) was examined by staining with 1:200 dilution of phalloidin-TRITC (Sigma-Aldrich, India) followed by confocal microscopy.

Pupal lethality assay: The numbers of larvae of different genotypes that pupated in a given cross were counted and the fate of these pupae was monitored. Pupae that died without differentiation or after differentiation and those that emerged as flies were also counted. In some cases, differentiated pupae

were classified as male and female, on the basis of the presence or the absence, respectively, of the sex comb that can be seen through the pupal case.

Acridine Orange assay for apoptosis: To assay the extent of apoptosis in third instar eye discs from larvae of desired genotypes, the discs were dissected in phosphate-buffered saline (PBS) (130 mM NaCl, 7 mM Na_2HPO_4, 3 mM KH_2PO_4, pH 7.2) and immediately stained with 1 μg Acridine Orange (AO)/ml of PBS for 3 min, following which the discs were washed twice with PBS, mounted in PBS (Spreij 1971), and viewed under a 10× objective of the LSM510 Meta Zeiss confocal microscope.

5-Bromo-4-chloro-3-indolyl-β-D-galactopyranoside staining of third instar larval eye discs: 5-Bromo-4-chloro-3-indolyl-β-D-galactopyranoside (X-gal) staining of *LacZ*-expressing third instar larval eye discs of the desired genotype(s) was performed as described earlier (Lakhotia *et al.* 2001).

Whole organ immunostaining and confocal microscopy: Eye discs from wandering third instar larvae of the desired genotypes were dissected and immunostained with the desired antibodies as described (Prasanth *et al.* 2000). The following primary antibodies were used: (1) 1:100 dilution of a rabbit active Caspase-3 antibody (Sigma, St. Louis), (2) 1:200 dilution of a polyclonal rabbit active JNK antibody (Promega, Madison, WI) for estimating the extent of JNK phosphorylation, 3) 1:100 dilution of the monoclonal rat elav-7E8A10 antibody (Developmental Studies Hybridoma Bank), (4) 1:10 dilution of the P11 mouse monoclonal antibody (Saumweber *et al.* 1980) for Hrb87F hnRNP, (5) 1:10 dilution of the Q18 mouse monoclonal antibody (Saumweber *et al.* 1980) for Hrb57A hnRNP, (6) 1:500 dilution of an affinity-purified rabbit β-galactosidase antibody (Molecular Probes, Eugene, OR), and (7) 1:500 or 1:250 dilution of an affinity-purified rabbit polyclonal αDIAP1 antibody (Lisi *et al.* 2000).

Appropriate secondary antibodies conjugated either with Cy3 (1:200, Sigma-Aldrich) or with Alexa Fluor 488 (1:200, Molecular Probes) were used to detect the given primary antibody. Chromatin was counterstained with 4′,6-diamidino-2-phenylindole dihydrochloride (DAPI) (1 μg/ml). Samples were examined on a Zeiss LSM 510 Meta laser scanning confocal microscope at appropriate settings using a plan-apo 40× or 63× oil immersion objective.

Reverse transcription–PCR: Total RNA was isolated from heads of adult flies of the desired genotype using TRIzol reagent per the manufacturer's (Sigma-Aldrich) instructions. First-strand cDNA was synthesized as described earlier (Mallik and Lakhotia 2009). One-tenth volume of the reaction mixture was subjected to PCR using hsrω-n-specific (forward primer 5′-GGCAGACATACGTACACGTGGAGCAT-3′ and reverse primer 5′-ACCAAGAGGCTAATCGAC-3′) and G3PDH primers (forward primer 5′-CCACTGCCGAGGAGGTCAACTA-3′ and reverse primer 5′-GCTCAGGGTGATTGCGTATGCA-3′). The thermal cycling program included an initial denaturation at 94° for 3 min followed by 35 cycles at 94° for 15 sec, at 60° for 30 sec, and at 72° for 30 sec. Final extension was carried out at 72° for 5 min. The PCR products were electrophoresed on a 2% agarose gel with appropriate molecular weight markers.

SDS–PAGE and Western blotting: To compare DIAP1 protein levels in different genetic backgrounds, extracts from adult heads of the genotypes *w; GMR-GAL4/+; GMR-rpr/+* and *w; GMR-GAL4/+; GMR-rpr/UAS-hsrω-RNAi*^{3}, respectively, were prepared and analyzed by SDS–PAGE and immunoblotting as described earlier (Prasanth *et al.* 2000). The primary antibodies used were 1:10,000 dilution of an affinity-purified rabbit polyclonal αDIAP1antibody and 1:200 dilution of mouse β-tubulin E7 antibody (Developmental Studies Hybridoma Bank). The immunoblots were developed with horseradish peroxidase-conjugated secondary antibody (1:1500 dilution of goat anti-mouse IgG or goat anti-rabbit IgG, Bangalore Genei, India) using an enhanced chemiluminescence detection system (Pierce, Rockford, IL). Blots were reprobed, as required, after stripping the earlier bound antibody by incubation in 100 mM 2-mercaptoethanol, 2% SDS, 62.5 mM Tris, pH 6.8, at 50° for 30 min.

Immunoprecipitation: Total cellular extracts of 50 pairs of wild-type or *GMR-GAL4*-driven *hsrω-RNAi*-expressing third instar eye discs were immunoprecipitated with the rabbit polyclonal αDIAP1 or the mouse monoclonal Hrb57A antibody, respectively, as described earlier (Prasanth *et al.* 2000). Approximately 1 μg of αDIAP1 and Hrb57A antibodies was used for each immunoprecipitation. Recovered proteins were resolved by SDS–PAGE and analyzed by Western blotting, using a 1:100 dilution of Hrb57A or Hrb87F antibodies or a 1:10,000 dilution of the αDIAP1 antibody.

All images were assembled using Adobe Photoshop 7.0.

RESULTS

As reported earlier (Mallik and Lakhotia 2009), among the several independent transgenic lines generated by us for targeted hsrω-RNAi, the *hsrω-RNAi*^{2} and *hsrω-RNAi*^{3} lines carry single insertions of the *UAS-hsrω-RNAi* transgene on chromosomes 2 and 3, respectively. In certain specific cases noted below, we also used another *hsrω-RNAi* transgenic line, *hsrω-RNAi(2X)*, which carries multiple tandem copies of the *hsrω-RNAi* transgene on chromosome 2. For targeted overexpression of the *hsrω* gene, two *EP* alleles, *i.e.*, *EP93D* and *EP3037* (Mallik and Lakhotia 2009), were used. As revealed by semiquantitative reverse transcription (RT)–PCR of total RNA derived from larval eye discs (Figure 1) expressing a single copy of the different *hsrω-RNAi* transgene insertions under control of the eye-specific *GMR-GAL4* driver, the *hsrω-RNAi(2X)* line showed maximum reduction (56.8% of wild type) in cellular levels of the hsrω transcripts while the *hsrω-RNAi*^{3} line was least effective (75.7%). Among the two EP lines, *GMR-GAL4*-driven expression of *EP3037* resulted in greater enhancement (146.4%) of hsrω transcript levels than following *EP93D* expression (111.2%) (Figure 1). Unless stated otherwise, most of the results relating to effects of depletion of hsrω transcripts in this article were obtained using the *hsrω-RNAi*^{3} transgene and in the following, *hsrω-RNAi* refers to the *hsrω-RNAi*^{3} transgene.

Modulation of hsrω transcript levels affects degeneration seen in eyes of *GMR-GAL4* homozygous adult flies: It is known (Kramer and Staveley 2003) that presence of two copies of the *GMR-GAL4* transgene results in a rough eye phenotype in adult flies (Figure 2, A and D; $N = 1943$) due to a high level of apoptotic cell death in larval eye discs (Figure 2J). Interestingly, depletion of hsrω-n RNA robustly suppressed the rough eye phenotype since eyes of *GMR-GAL4/GMR-GAL4; hsrω-RNAi/hsrω-RNAi* flies (Figure 2, B and E; $N = 2365$) were indistinguishable from those of wild-type flies (not

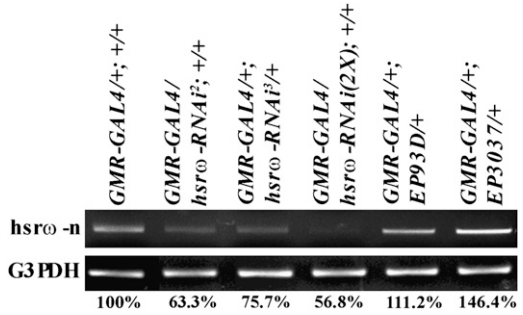

FIGURE 1.—GAL4-driven expression of the *hsrω-RNAi* transgene or the *EP* alleles modulates cellular levels of hsrω transcripts. Semiquantitative RT–PCR with total RNA from adult heads of different genotypes, indicated above each lane, shows that GAL4-driven expression of the different *hsrω-RNAi* transgenes varyingly depletes cellular levels of the hsrω-n RNA with maximum depletion seen in the *GMR-GAL4/hsrω-RNAi(2X)* genotype while expression of any of the *EP* (*EP93D* or *EP3037*) alleles of the gene enhances hsrω transcript levels. G3PDH amplicons in each sample were used as a loading control. The percent value below each lane indicates the relative levels of the hsrω-n RNA in different genotypes.

shown). On the other hand, augmentation of hsrω transcript levels in *GMR-GAL4/GMR-GAL4; EP93D/EP93D* homozygotes enhanced the eye damage, resulting in highly disorganized ommatidial arrays (Figure 2, C and F; $N = 2401$). It should be noted that no discernible eye phenotype was seen in adult flies carrying a single copy of the *GMR-GAL4* driver alone or in conjunction with one or two copies of *hsrω-RNAi* or the *EP* alleles (not shown).

Phalloidin staining of freshly eclosed *GMR-GAL4* homozygous adult fly heads ($N = 6$) revealed degeneration of photoreceptor neurons (Figure 2G). Expression of *hsrω-RNAi* in a *GMR-GAL4* homozygous background markedly suppressed this degeneration (Figure 2H) since the majority of the ommatidia in eyes of these flies ($N = 6$) showed the characteristic seven photoreceptor rhabdomeres in near normal pattern. In contrast, increased levels of hsrω transcripts due to *GMR-GAL4*-driven expression of *EP93D* exacerbated the phenotype since photoreceptors were almost completely missing from ommatidia (Figure 2I; $N = 6$).

We also assessed the level of apoptosis in third-instar larval eye discs of different genotypes by AO staining, which identifies dying cells. Consistent with the observed adult eye phenotypes, AO positive cells were nearly absent in *hsrω-RNAi* expressing *GMR-GAL4* homozygous discs (Figure 2K; $N = 8$) while their number was significantly greater in *hsrω* overexpressing (Figure 2L; $N = 10$) eye discs than in those expressing two copies of *GMR-GAL4 per se* (Figure 2J; $N = 8$).

Misexpression of the *hsrω* gene modulates cell death caused by the RHG family of proteins: Since the above results suggested that modulation of hsrω transcript levels affected cell death in Drosophila, we examined the effects of reduced or enhanced levels of hsrω transcripts on apoptosis triggered by ectopic expression of RHG proteins, the key activators of the caspase-mediated apoptosis (VERNOOY *et al.* 2000).

As reported earlier (GOYAL *et al.* 2000; SONG *et al.* 2000) and seen in Figure 3, A, E, I, M, Q, and U, ectopic expression of any of the RHG proteins under control of the *GMR* promoter caused massive cell death in the developing eye discs, resulting in highly ablated and abnormally shaped eyes, with the most pronounced damage seen in flies expressing *GMR-hid* (Figure 3, I and M, $N = 424$), with *GMR-Rpr* ($N = 459$) and *GMR-Grim* ($N = 482$) resulting in progressively less damage, respectively. Coexpression of a single copy of the *hsrω-RNAi* transgene significantly rescued Reaper ($N = 457$)- or Grim ($N = 498$)-mediated small and damaged eye phenotypes (Figure 3, compare A, E, Q, and U with B, F, R, and V, respectively). However, depletion of hsrω-n RNA had only a marginal effect on the *GMR-hid* ($N = 432$)-induced extensive damage (Figure 3, compare I and M with J and N). Increased hsrω transcript levels following *EP93D* or *EP3037* expression enhanced the severely ablated eye phenotypes caused by overexpression of Rpr ($N = 480$) or Grim ($N = 460$) proteins in developing eyes while in the case of Hid ($N = 474$) the damage was already very extensive and therefore, aggravation, if any, was not as discernible (Figure 3, compare A, E, I, M, Q, and U with C, G, K, O, S, and W). In accordance with the above, *GMR-GAL4*-mediated simultaneous expression of any of the *EP* alleles and the *hsrω-RNAi* transgene in *GMR-rpr* or *GMR-grim* backgrounds not only eliminated the enhancing effect of the *EP93D* or *EP3037* alleles but also reversed the level of degeneration caused by expression of Rpr or Grim alone such that eyes of *GMR-GAL4/+; GMR-rpr/hsrω-RNAi EP3037* (Figure 3, D and H; $N = 463$) or *GMR-GAL4/+; GMR-grim/hsrω-RNAi EP3037* (Figure 3, T and X; $N = 405$) flies showed somewhat less degeneration than seen in *GMR-GAL4/+; GMR-rpr/+* (Figure 3, A and E) or *GMR-GAL4/+; GMR-grim/+* flies (Figure 3, Q and U). This confirmed that the modulation of Reaper- or Grim-induced eye phenotypes by *EP93D* or *EP3037* or *hsrω-RNAi* transgenes was indeed due to alterations in the levels of the hsrω transcripts in developing eyes.

Loss of hsrω transcripts ameliorates apoptosis caused by expression of full-length as well as processed caspases: As noted earlier, the primary proapoptotic function of the RHG proteins is to liberate caspases like DRONC from DIAP1 inhibition (ARYA *et al.* 2007). The activated DRONC initiates a proteolytic cascade that culminates in cell death. Therefore, we investigated if *hsrω-RNAi* had any effect on cell death caused by overexpression of full-length [*UAS-pro-dronc*^{W} (weak) or *UAS-pro-dronc*^{S} (strong)] or processed (*UAS-ΔN dronc*) caspases.

GMR-GAL4-driven ectopic expression of *UAS-pro-dronc*^{W} ($N = 524$) resulted in adult eyes with apparently

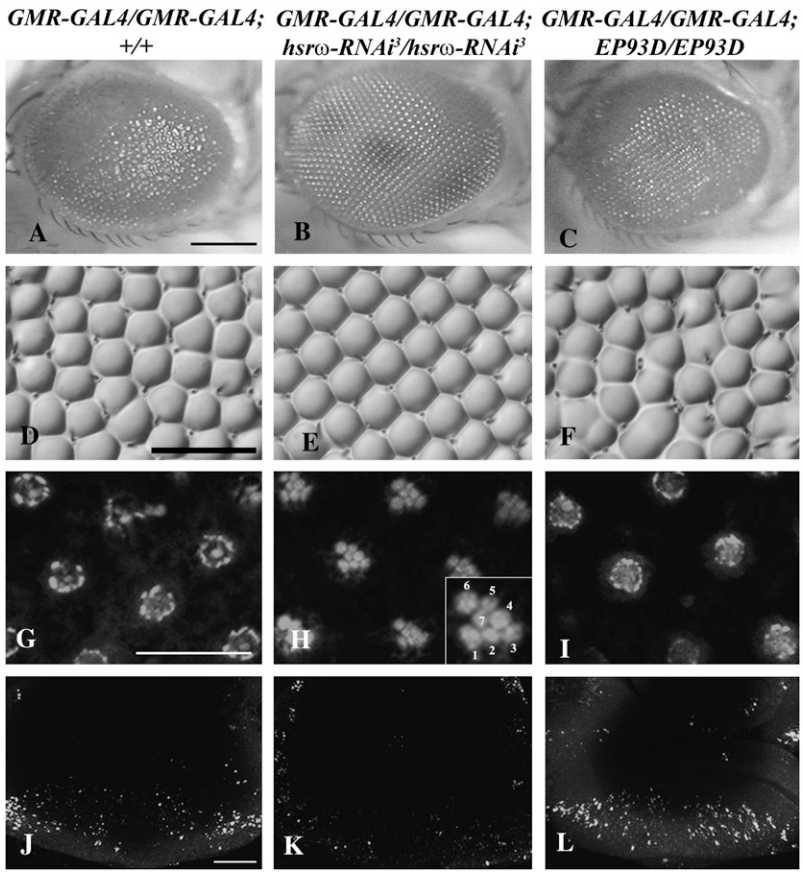

FIGURE 2.—hsrω transcript levels modulate eye degeneration seen in *GMR-GAL4* homozygous flies. Genotypes are indicated on top of each column. (A–C) Light micrographs of adult eyes; (D–F) nail polish imprints of the eye surface; (G–I) confocal projections of phalloidin-stained eyes; (J–L) images of AO-stained live third instar larval eye discs. Inset in H shows the asymmetrical arrangement of the seven rhabdomeres (1–7) in a single ommatidium from a *GMR-GAL4/GMR-GAL4; hsrω-RNAi/hsrω-RNAi* adult eye as characteristically seen in wild-type eyes. Such regular arrangement is absent in ommatidia from eyes of *GMR-GAL4/GMR-GAL4; +/+* (G) as well as *GMR-GAL4/GMR-GAL4; EP93D/EP93D* (I) flies. Bars: for A–C in A, D–F in D, G–I in G, 20 μm; and for J–L in J, 50 μm.

normal external morphology and size (Figure 4, A and B) but with internal ablation of most photoreceptor and pigment cells because of which the pseudopupil image was not formed (not shown). Even though these flies were genetically w^+, their eyes showed only very small patches of red pigmentation (Figure 4A). Expression of *pro-dronc*^{S} ($N = 58$) and Δ*N dronc* ($N = 34$) transgenes using the *GMR-GAL4* driver resulted in more severely malformed and depigmented adult eyes (Figure 4, E and F, and Figure 4, I and J, respectively). Interestingly, downregulation of hsrω-n transcripts mitigated the spotted/ablated eye phenotypes caused by directed expression of either the weak (Figure 4, C and D; $N = 1464$) or the strong full-length *dronc* (Figure 4, G and H; $N = 388$) or the processed Δ*N dronc* (Figure 4, K and L; $N = 1822$) transgene. External morphology of eyes of flies expressing the various *dronc* transgenes in the presence of the *hsrω-RNAi* transgene was essentially similar to that of wild-type flies (Figure 4, D, H, and L).

As already reported (MEIER *et al.* 2000), the majority of the progeny expressing *pro-dronc*^{S} or Δ*N dronc* under control of *GMR-GAL4* at 25° failed to eclose out of the pupal case because of extreme head malformations. As a consequence, such flies die trapped in their pupae cases. When raised at 18°, a few flies (58 *GMR-GAL4/+; UAS-pro-dronc*^{S}*/+* flies of 1036 and 34 *GMR-GAL4/+; UAS-*Δ*N dronc/+* flies of 1193 differentiated pupae examined) emerged with completely ablated eyes and reduced head size (Figure 4, E, F, I, and J). In contrast, heads of flies coexpressing *hsrω-RNAi* and *UAS-pro-dronc*^{S} (strong) or *hsrω-RNAi* and *UAS-*Δ*N dronc* were normal, resulting in dramatic rescue of pupal lethality. *GMR-GAL4*-driven coexpression of *hsrω-RNAi* and *UAS-pro-dronc*^{S} resulted in 100% ($N = 310$) rescue of lethality in females but only 21.9% (78/356) of male progeny eclosed. Coexpression of *hsrω-RNAi* in concert with the activated *dronc* transgene also enhanced emergence of adult flies to 90.5% ($N = 2013$, Table 1).

Immunostaining of third instar larval eye-imaginal discs expressing Δ*N dronc* alone ($N = 8$) or in conjunction with *hsrω-RNAi* ($N = 6$) with an active caspase-3 antibody, which detects the Drosophila effector caspase DrICE, revealed that compared to the robust staining (Figure 4, M and N) seen in larval eye discs expressing Δ*N dronc*, caspase-3 activity (activated DrICE) was largely suppressed in discs coexpressing *hsrω-RNAi* with Δ*N dronc* (Figure 4, compare O and P with M and N, respectively).

We further examined if hsrω-n RNAi modulates cell death caused by overexpression of the activated (N-terminal prodomain removed) effector caspase Dcp-1 using the *GMR-*Δ*N-dcp-1* transgenic line (SONG *et al.* 2000). Expression of *GMR-*Δ*N-dcp-1* caused complete loss of ommatidial integrity (Figure 4, Q and R) and death of ~51.7% differentiated pupae (Table 1). Coexpression of *hsrω-RNAi*, however, nearly completely re-

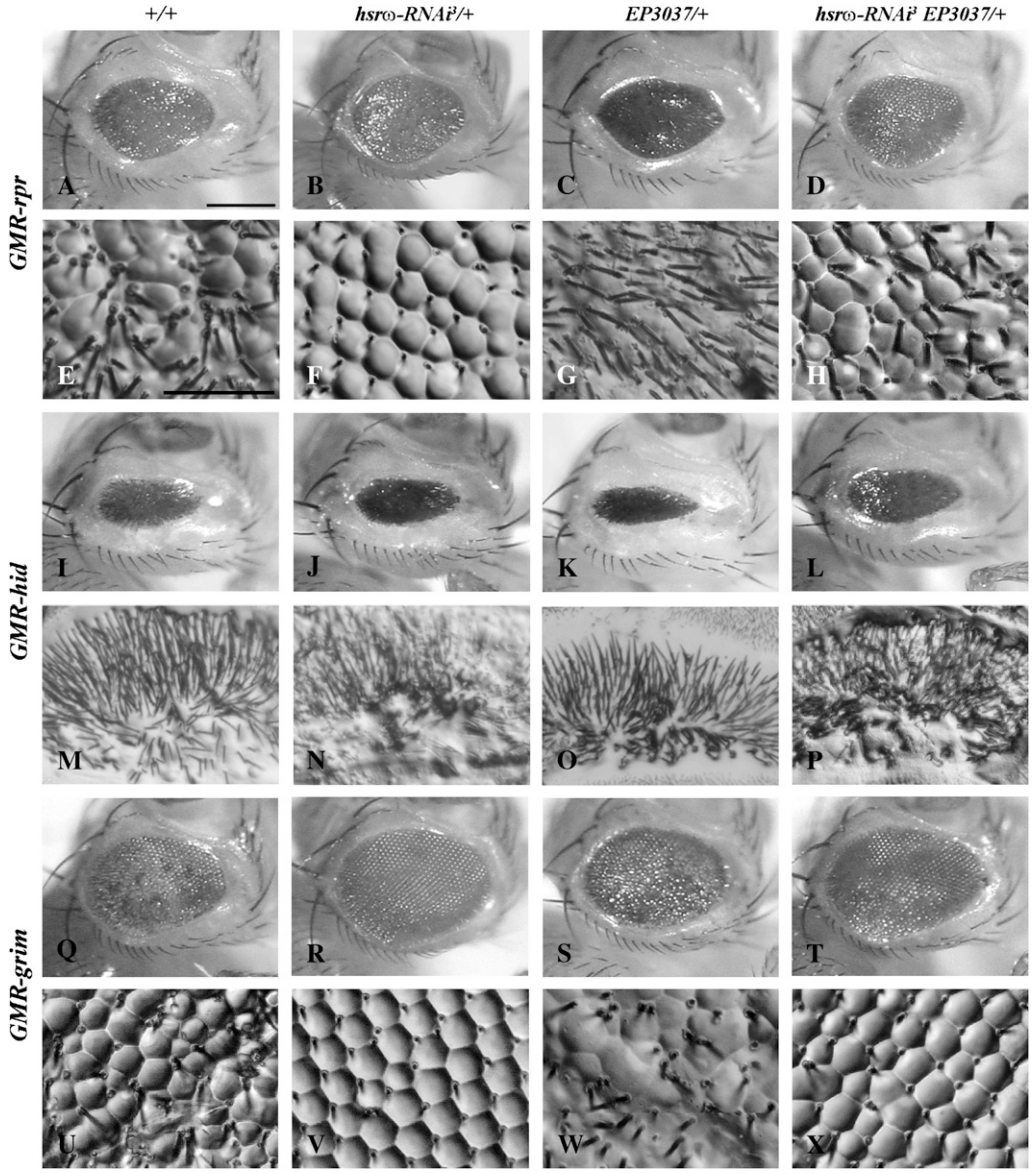

FIGURE 3.—Downregulation of hsrω transcript levels ameliorates eye degeneration caused by ectopic expression of the RHG proteins in Drosophila. Genotypes common to rows are indicated on the left while those for columns are indicated on top. A–D, I–L, and Q–T are photomicrographs and E–H, M–P, and U–X are nail polish imprints of eyes of adults of the indicated genotypes. Bars: for A–D, I–L, and Q–T in A and for E–H, M–P, and U–X in E, 20 μm.

stored the regular arrangement of ommatidial arrays (Figure 4T) and external eye pigmentation (Figure 4S). Furthermore, pupal lethality was also suppressed since only 12% died as fully differentiated pharates (Table 1). Thus, *hsrω* appears to act upstream of initiator and effector caspases and its depletion prevents activation of caspase-3.

Effect of hsrω transcript levels on DIAP1-RNAi-mediated cell death in Drosophila: In view of the suppression of Drosophila apical as well as effector caspases by DIAP1 (LEULIER *et al.* 2006; ARYA *et al.* 2007), depletion of DIAP1 levels by *GMR-GAL4*-driven expression of the *UAS-DIAP1-RNAi* transgene in eye discs induced massive degeneration reflected in disrupted pigmentation and reduction and severe roughening of the eye (Figure 5, A, B, H, and I). Intriguingly, flies expressing the *UAS-DIAP1-RNAi* transgene in a homozygous w^- background (Figure 5, B and I, *w/w; GMR-GAL4 UAS-DIAP1-RNAi/+*) exhibited a more severely degenerated eye phenotype than those expressing *DIAP1-RNAi* in a w^+ heterozygous background (Figure 5, A and H, w^+/w; *GMR-GAL4 UAS-DIAP1-RNAi/+*). Since all the transgenic stocks used in the present study were homozygous for the w^- allele on the X chromosome, we used the eye morphology of the *w/w; GMR-GAL4 UAS-DIAP1-RNAi/+* as our experimental control. Interestingly, unlike the above results, flies expressing a single copy of the third chromosomal *hsrω-RNAi* transgene had little or only a marginal restorative effect (Figure 5, C and J) on *DIAP1-RNAi*-induced eye degeneration. Coexpression of *DIAP1-RNAi* with one copy of the *hsrω-RNAi²* (MALLIK and LAKHOTIA 2009) transgene improved the eye morphology slightly more than the third chromosomal *hsrω-RNAi* transgene (Figure 5, D and K; $N = 491$). Still better recovery of eye size and morphology was seen

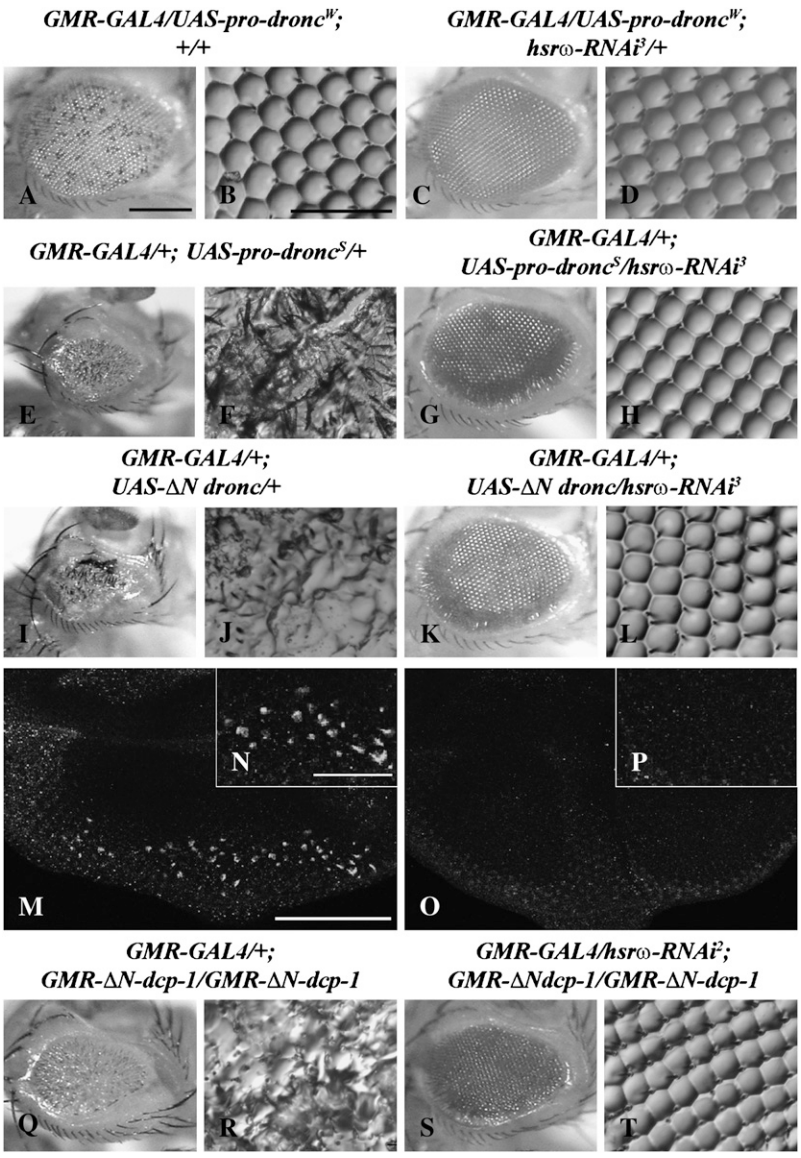

FIGURE 4.—Depletion of hsrω-n transcripts effectively suppresses cell death caused by directed expression of initiator or effector caspases. A, C, E, G, I, K, Q, and S are light micrographs of adult eyes and B, D, F, H, J, L, R, and T are nail polish imprints of the eye surface from flies of different genotypes as indicated on the top of each row. M–P are confocal projections of eye discs from *GMR-GAL4/+; UAS-ΔN dronc/+* (M and N) and *GMR-GAL4/+; UAS-ΔN dronc/hsr*ω*-RNAi* (O and P) third instar larvae immunostained with the active Caspase-3 antibody. N and P are higher magnification images of the basal regions of discs shown in M and O, respectively. Bars: for A, C, E, G, I, K, Q, and S in A, for B, D, F, H, J, L, R, and T in B, and for N and P in N, 20 μm; and for M and O in M, 50 μm, respectively.

when the *hsr*ω*-RNAi(2X)* transgenic line, carrying tandem insertions of the transgene, was used (Figure 5E; $N = 638$). However, it is significant that the regular ommatidial lattice in the eyes was still disrupted (Figure 5L). Augmentation of hsrω transcript levels using the *EP93D* (Figure 5, F and M; $N = 382$) and the *EP3037* (Figure 5, G and N; $N = 344$) alleles led to a slight enhancement of the eye degeneration compared to that seen in *DIAP1-RNAi*-expressing adult flies.

Data presented in Table 2 show that like the eye damage, lethality at the differentiated pupal stage following *GMR-GAL4*-driven expression of *UAS-DIAP1-RNAi* was also differentially suppressed by different *hsr*ω*-RNAi* lines. Further, as in the case of eye degeneration, *GMR-GAL4*-driven expression of *UAS-DIAP1-RNAi* caused much less pupal lethality in a w^{+}/w (5.5%, Table 2) than in a *w/w* (48.2%, Table 2) background. Coexpression of the different *hsr*ω*-RNAi* transgenes suppressed pupal lethality in accordance with their recovery of the eye morphology (Table 2). Surprisingly, however, coexpression of either *EP3037* or *EP93D* showed varying levels of rescuing effect on DIAP1-RNAi-mediated pupal lethality unlike the slight enhancement of DIAP1-RNAi-induced eye degeneration in both cases. While coexpression of *EP3037* in the DIAP1-depleted background did not affect the frequency of dying pupae (Table 2), coexpression of *EP93D* and *DIAP1-RNAi* increased the eclosion of *w/w; GMR-GAL4 UAS-DIAP1-RNAi/EP93D* flies (Table 2**)**. The differences observed in the efficiency of rescue achieved by the *EP93D* or the *EP3037* transgenes in the various mutant backgrounds most likely reflect variations in the local chromatin environment of the *EP*-transposon insertion sites that may affect hsrω expression differently (MALLIK and LAKHOTIA 2009).

Downregulation of hsrω transcripts fails to suppress induced apoptosis in the DIAP1-RNAi background: As already reported (HAY *et al.* 1995), augmentation of

TABLE 1

Modulation of caspase-mediated pupal lethality by downregulation of the hsrω transcripts in Drosophila

Genotype	No. of pupae examined	No. (%) of differentiated pupae dying[a]		No. (%) of males eclosing	No. (%) of females eclosing
		Male	Female		
GMR-GAL4/+;UAS-pro-dronc^c/+	1036	546 (52.7)	432 (41.7)	7 (0.7)	51 (4.9)
GMR-GAL4/+;UAS-pro-dronc^c/hsrω-RNAi^3	666	278 (41.7)	0	78 (11.7)	310 (46.5)
GMR-GAL4/+;UAS-ΔN dronc/+	1193	549 (46.0)	610 (51.1)	23 (1.9)	11 (0.9)
GMR-GAL4/+;UAS-ΔN dronc/hsrω-RNAi^3	2013	174 (8.6)	17 (0.8)	815 (40.5)	1007 (50.0)
hsrω-RNAi^2/+; GMR-ΔN-dcp-1/GMR-ΔN-dcp-1	431	223 (51.7)[b]		94 (21.8)	114 (26.5)
GMR-GAL4/hsrω-RNAi^2; GMR-ΔN-dcp-1/GMR-ΔN-dcp-1	274	33 (12.0)[b]		131 (47.8)	110 (40.1)

[a] Numbers in parentheses indicate percentage of total pupae examined.
[b] Male and female dying pupae not counted separately in these crosses.

DIAP1 levels (Figure 6, A and G; $N > 250$ in each case) in developing eyes rescued the small eye phenotypes caused by overexpression of the RHG proteins. Coexpression of a single copy of the *hsrω-RNAi* transgene further improved the eye morphology and size such that the eyes of *GMR-GAL4/hsrω-RNAi^2; GMR-rpr/UAS-DIAP1* (Figure 6, B and H; $N = 235$) flies could not be distinguished from those of wild-type flies. On the other hand, as reported earlier (Leulier *et al.* 2006), we also observed that RNAi-mediated downregulation of endogenous DIAP1 levels enhanced the eye damage caused by expression of *GMR-rpr* (compare Figure 6, C and I, with Figure 3, A and E; $N = 206$) or *GMR-grim* (compare Figure 6, E and K, with Figure 3, Q and U; $N = 219$). Interestingly, unlike the above-noted suppression of eye damage by coexpression of the *hsrω-RNAi* transgene in *GMR-rpr* or *GMR-grim* backgrounds (Figure 3), expression of one copy of the *hsrω-RNAi* transgene failed to suppress eye damage caused by coexpression of *GMR-rpr* (Figure 6, D and J; $N = 198$) or *GMR-grim* (Figure 6, F and L; $N = 213$) with *UAS-DIAP1-RNAi*. These results, together with those presented in the previous section, strongly suggest that presence of DIAP1 is necessary for the inhibitory effect of reduced levels of hsrω transcripts on induced apoptosis.

hsrω transcripts regulate cellular levels of DIAP1 through its association with the hnRNP, Hrb57A: With a view to understand the basis of the above-noted genetic interactions between hsrω transcripts and DIAP1, we immunostained eye discs of various genotypes to examine the distribution of DIAP1 and some of the hnRNPs, *i.e.*, Hrb57A and Hrb87F, that are associated with the hsrω transcripts. It is interesting that Hrb57A (hnRNP K homolog, Charroux *et al.* 1999), which is also known to affect apoptosis in imaginal disc cells (Charroux *et al.* 1999), was found to significantly colocalize with DIAP1, especially in the cytoplasm.

In wild-type third instar larval eye discs ($N = 10$), DIAP1 was present as distinct cytoplasmic and nuclear granules as well as in a diffuse manner in the cytoplasm (Figure 7A). Hrb57A was also present in nuclei of the photoreceptor cells in a diffuse and speckled pattern (Figure 7, A′ and K). In addition, distinct cytoplasmic granules of Hrb57A were also present in these cells and, significantly, the cytoplasmic Hrb57A granules were

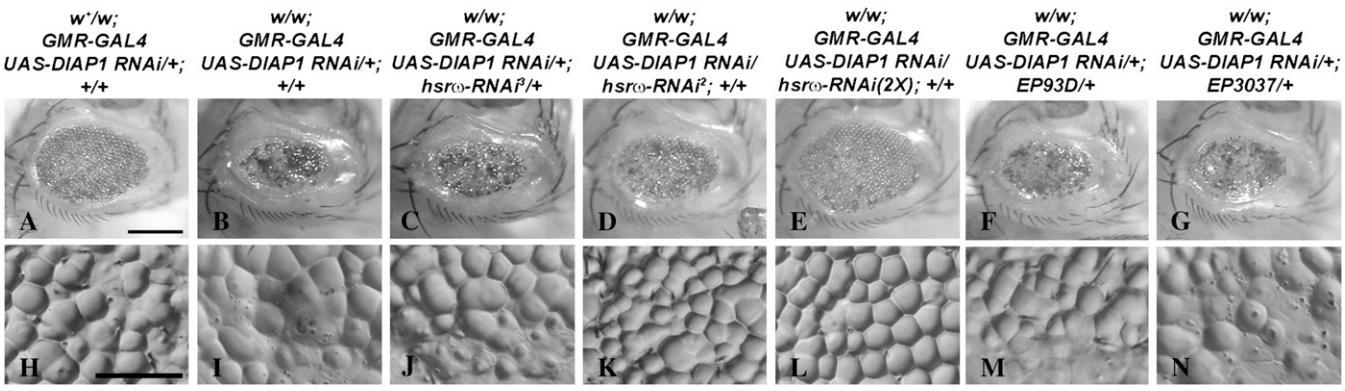

Figure 5.—The extent of DIAP1-RNAi-mediated eye degeneration varies in w^+ and w^- backgrounds and downregulation of hsrω-n RNA, with any one of the three different *hsrω-RNAi* transgenes, has little or only a marginal effect on apoptosis following DIAP1-RNAi. Genotypes are indicated on top of each column. (A–G) Photomicrographs of adult eyes; (H–N) nail polish imprints of the eye surface. Bars, 20 μm.

TABLE 2

Modulation of DIAP1-RNAi-mediated pupal lethality by altered levels of the endogenous hsrω transcripts in Drosophila

Genotype	*N*	% pupation	Pupal differentiation	% adult emergence
w^{+}*/w; GMR-GAL4 UAS-DIAP1-RNAi/+; +/+*	2020	100	2.3% die during pupal development 3.2% die after differentiation	94.5
w/w; GMR-GAL4 UAS-DIAP1-RNAi/+; +/+	1523	100	2.8% progeny do not differentiate 45.4% die as differentiated pupae	51.8
w/w; GMR-GAL4 UAS-DIAP1-RNAi/+; hsrω-RNAi^{3}*/+*	1948	100	0.6% die during pupal development 50.6% die after differentiation	48.8
w/w; GMR-GAL4 UAS-DIAP1-RNAi/hsrω-RNAi^{2}*; +/+*	505	100	2.8% die as differentiated pupae	97.2
w/w; GMR-GAL4 UAS-DIAP1-RNAi/hsrω-RNAi(2X); +/+	642	100	100% pupae differentiate	99.4
w/w; GMR-GAL4 UAS-DIAP1-RNAi/+; EP93D/+	486	100	21.4% die as differentiated pupae	78.6
w/w; GMR-GAL4 UAS-DIAP1-RNAi/+; EP3037/+	655	100	47.5% die after differentiation	52.5

often adjacent to or partially or fully overlapped with those of DIAP1 (Figure 7, A′ and K). In *w/w;+/+; +/+* larval eye discs ($N = 6$, Figure 7B), the overall diffuse as well as granular cytoplasmic DIAP1 staining was significantly less than that in *w*$^{+}$*/w*$^{+}$*; +/+; +/+* eye discs (compare Figure 7A with 7B). Furthermore, the nuclear and cytoplasmic clusters of Hrb57A were clearly more prominent in the *w/w; +/+; +/+* eye discs (Figure 7, B′ and L). Although the number of cytoplasmic Hrb57A granules/speckles in such eye discs was less than in the *w*$^{+}$*/w*$^{+}$*; +/+; +/+* discs, they were larger in size (compare Figure 7A′ with 7B′). The distribution of DIAP1 and Hrb57A proteins in *w/w; GMR-GAL4/+; +/+* eye discs ($N = 5$, Figure 7M) was more or less comparable to that in wild-type eye discs (Figure 7K). Compared to the *w/w; GMR-GAL4/+; +/+* larval eye discs, those of *w/w; GMR-GAL4/GMR-GAL4; +/+* ($N = 6$) showed significantly reduced levels of the granular form of DIAP1 (Figure 7D). The nuclear distribution of Hrb57A was slightly enhanced in the developing ommatidial units in *w/w; GMR-GAL4/GMR-GAL4; +/+* eye discs although the cytoplasmic granules appeared less frequent (Figure 7D′) than in *w/w; GMR-GAL4/+; +/+* and more so when compared with the *w/w; +/+; +/+* larval eye discs (Figure 7, C′ and B′).

Interestingly, *GMR-GAL4*-driven expression of the *hsrω-RNAi* transgene (*w/w; GMR-GAL4/GMR-GAL4; hsrω-RNAi/hsrω-RNAi*) resulted in significant changes in the distribution of Hrb57A and DIAP1. The granular form of DIAP1 in these discs ($N = 11$; Figure 7, E′ and O) appeared similar to that in wild-type discs (Figure 7, A and K). Nuclear granules of Hrb57A (Figure 7, E′ and O) were no longer visible in *hsrω-RNAi*-expressing photoreceptor cells but the cytoplasmic granules (Figure 7, E′ and O) were much more abundant and showed a greater overlap with the DIAP1 granules following expression of *hsrω-RNAi* (Figure 7O). Significantly, the *w/w; GMR-GAL4/GMR-GAL4; hsrω-RNAi/hsrω-RNAi* eye discs showed less nuclear Hrb57A while the cytoplasmic granules were more abundant.

Augmentation of hsrω transcript levels using either two copies of *EP93D* ($N = 6$) or a single copy of the *EP3037* ($N = 5$) allele also resulted in significant changes in the distribution of Hrb57A and DIAP1. Intriguingly, the cytoplasmic DIAP1 granules in the *EP*-expressing discs (Figure 7, F and P, and Figure 7, G and Q) were more prominent than in those expressing two copies of the *GMR-GAL4* transgene alone (Figure 7, D and N) but these were smaller than those seen in *w/w; GMR-GAL4/GMR-GAL4; hsrω-RNAi/hsrω-RNAi* eye discs (Figure 7, E and O). Prominent nuclear clusters of Hrb57A were seen in the *EP93D* (Figure 7, F′ and P)- and *EP3037* (Figure 7, G and Q)-expressing discs.

Ectopic expression of the apical cell death trigger Rpr in developing eye discs ($N = 6$) under control of the eye-specific *GMR* promoter led to almost complete absence of the diffuse staining for DIAP1 as well as Hrb57A (Figure 7, H and H′). Interestingly, the residual DIAP1 and Hrb57A proteins in *w/w; GMR-GAL4/+; GMR-rpr/+* discs were present mostly as granules displaying a much greater colocalization (Figure 7R) than seen in wild-type or *w/w; +/+; +/+* or *w/w; GMR-GAL4/+; +/+* eye discs. Coexpression of a single copy of *hsrω-RNAi* in eye discs expressing *GMR-rpr* ($N = 7$) led to a significantly enhanced diffuse nuclear staining for both DIAP1 and Hrb57A (Figure 7, I and I′). The DIAP1 as well as Hrb57A granules in these discs were smaller and more like those seen in wild-type discs (compare Figure 7S with 7K). *GMR-GAL4*-driven expression of a single copy of *EP3037* in the Rpr-expressing discs ($N = 11$) resulted in a high reduction of the Hrb57A levels (Figure 7J′) while the pattern of DIAP1 in these discs (Figure 7, J and T) was more or less similar to that seen in the *w/w; +/+; GMR-rpr/+* eye discs (Figure 7, H and R).

We also examined the distribution of DIAP1 in relation to Hrb87F, a homolog of hnRNPA1 (Haynes *et al.* 1991), by co-immunostaining eye discs from third instar larvae of different genotypes (Figure 8). The cellular distribution of Hrb87F was also affected by the hsrω transcript levels, but unlike Hrb57A, Hrb87F

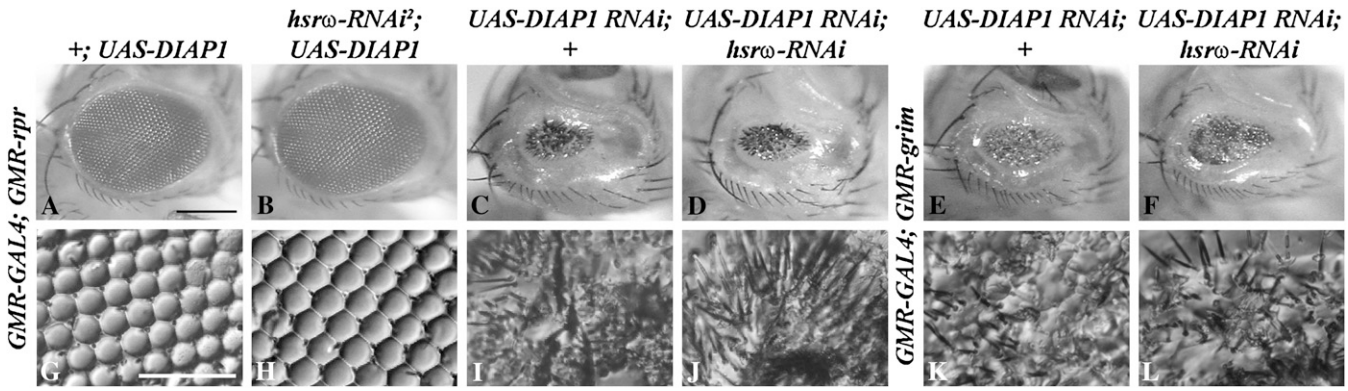

FIGURE 6.—DIAP1-RNAi-mediated enhancement of Rpr- or Grim-induced cell killing is not reversed by downregulation of hsrω transcripts. (A–F) Photomicrographs of eyes; (G–L) nail polish imprints of the eye surface. Genotype common to the rows is indicated on the left while those for columns are indicated on top. Bars: for A–F in A and G–L in G, 20 μm.

showed much less colocalization with DIAP1. In *w/w; GMR-GAL4/GMR-GAL4; +/+* discs ($N = 5$), Hrb87F, like Hrb57A, showed a diffuse as well as speckled distribution (Figure 8, B and C), but the cytoplasmic granules of this protein were less abundant and, when present, were generally smaller than those of Hrb57A (Figure 7D′). In *hsrω-RNAi*-expressing eye discs ($N = 7$), the nuclear speckles of Hrb87F disappeared (Figure 8 E and F) but unlike Hrb57A (Figure 7, E′ and O), they did not display as frequent association or overlap with the cytoplasmic DIAP1 granules. Overexpression of hsrω transcripts in *w/w; GMR-GAL4/GMR-GAL4; EP93D/EP93D* ($N = 6$, Figure 8H) or in *w/w; GMR-GAL4/GMR-GAL4; EP3037/+* ($N = 5$, Figure 8K) resulted in a greater nuclear accumulation of Hrb87F but the Hrb87F and DIAP1 proteins remained largely independent of each other (Figure 8, I and L).

The above changes in DIAP1 levels and the apparent association between DIAP1 and Hrb57A were confirmed by Western blotting and immunoprecipitation. Comparison of the levels of DIAP1 in Western blot (Figure 8M) of total proteins from *GMR-GAL4/+; GMR-rpr/+* (lane 1) or *GMR-GAL4/+; GMR-rpr/hsrω-RNAi* (lane 2) adult eyes showed that compared to flies expressing *GMR-rpr* alone, the DIAP1 level in *hsrω-RNAi* coexpressing adult flies was considerably higher. Further, as shown in Figure 8N, immunoprecipitation of eye disc proteins with the αDIAP1 antibody pulled down Hrb57A (lanes 1 and 2), more so in eye discs from *GMR-GAL4; hsrω-RNAi/hsrω-RNAi* larvae (lane 2) than in those from wild type (lane 1). In accordance with these results, immunoprecipitation with anti-Hrb57A also consistently pulled down DIAP1 (Figure 8N, lanes 5 and 6), demonstrating that these proteins are physically associated and thus likely to interact directly or within a complex.

In agreement with the above immunostaining results, the Hrb87F protein was not detectable in anti-αDIAP1 immunoprecipitates from eye discs of any of the genotypes (Figure 8O).

Altered levels of hsrω transcripts affect apoptosis induced by expression of the stress-activated protein kinase, JNK: Among the mitogen-activated protein (MAP) kinase cascades, the extracellular signal-related kinases (ERKs) play a central role in survival and mitogenic signaling, while JNKs and p38 MAP kinases are preferentially activated by environmental stresses and are actively involved in various stress responses including cell death, survival, and differentiation (KYRIAKIS and AVRUCH 2001; STRONACH 2005). To determine if the suppression of induced apoptosis following depletion of hsrω transcripts also involved the JNK, p38 MAP kinase, and/or EGF receptor (EGFR) signaling cascades, we tested genetic interactions between single copies of the *hsrω-RNAi* transgene or the *EP* alleles of *hsrω* and various transgenes that alter the expression of these pathways. Altered levels of hsrω transcripts had no effect on eye phenotypes caused by overexpression of p38 MAP kinase (not shown) or EGFR (see below). However, the JNK signaling cascade was affected by modulation of hsrω transcript levels.

Eiger (Egr), a type II membrane protein belonging to the TNF superfamily of ligands, activates the JNK signaling cascade (IGAKI *et al.* 2002; MORENO *et al.* 2002). As reported earlier (IGAKI *et al.* 2002; MORENO *et al.* 2002), *GMR-GAL4*-driven ectopic expression of wild-type Eiger in the developing eye discs of Drosophila triggered massive apoptosis, resulting in almost complete loss of the eye in adult flies (Figure 9, A and E; $N = 1653$) and lethality of ~36.2% differentiated pupae (Table 3). Downregulation of hsrω-n RNA level with one copy of *hsrω-RNAi* not only strongly suppressed (Figure 9B; $N = 1716$) the Eiger-induced apoptosis and restored the ommatidial integrity (Figure 9F) to almost that seen in wild-type flies but also substantially reduced mortality of differentiated *GMR-GAL4/UAS-egr; hsrω-RNAi/+* pupae (Table 3). Increased expression of hsrω transcripts, however, enhanced the phenotype leading to severe head malformations and the formation of black lesions on the eye (Figure 9, C and G, $N = 800$; and

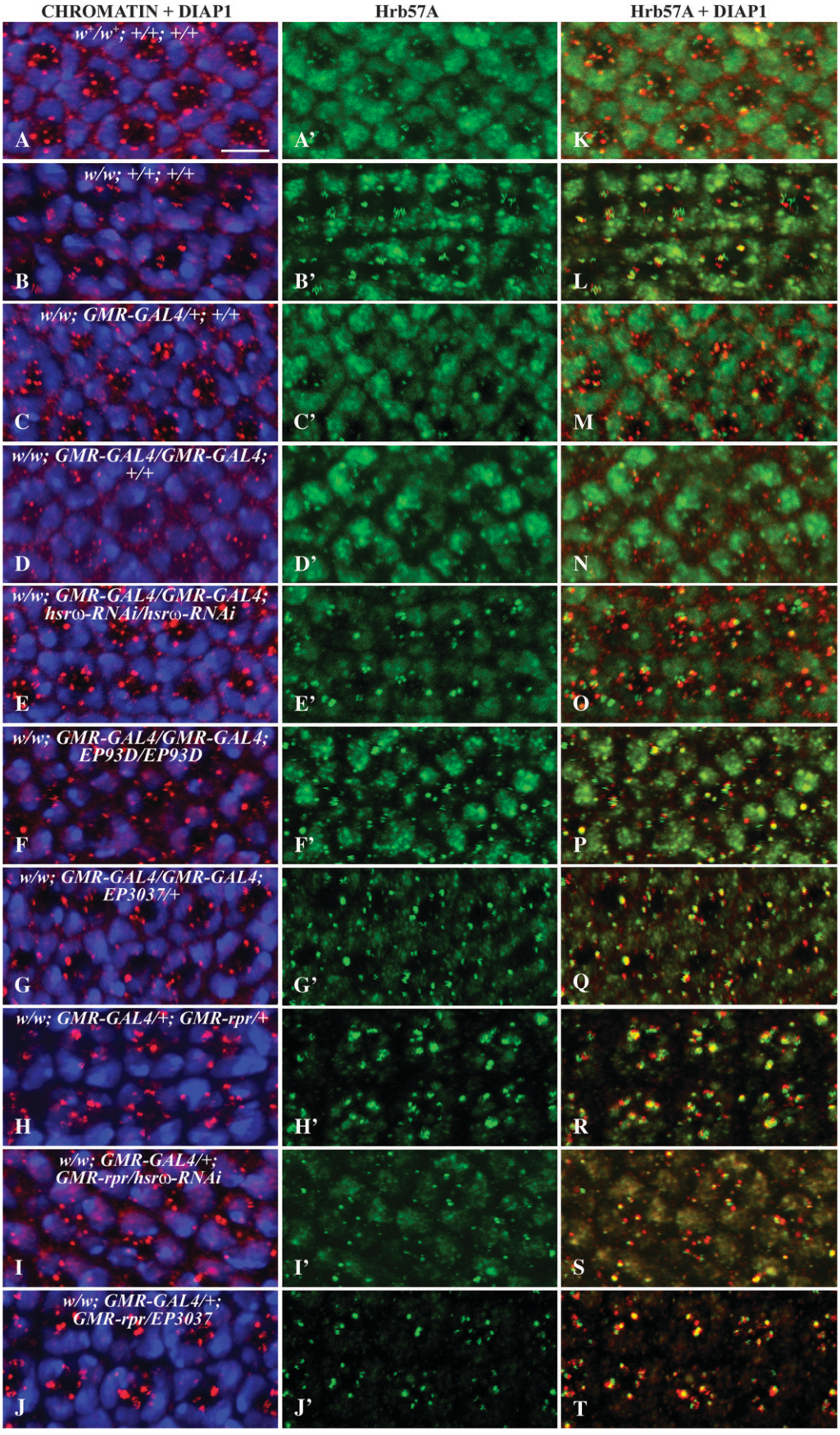

FIGURE 7.—DIAP1 physically associates with the hnRNP, Hrb57A. Projections of confocal images of late third instar larval eye discs are shown (genotype for each row is indicated in the first column) immunostained with anti-αDIAP1 (red, A–J) and anti-Hrb57A (green, A′–J′) and counterstained with 4′,6-diamidino-2-phenylindole dihydrochloride (DAPI) (blue, A–J). Merged images of DIAP1- and DAPI-stained nuclei are shown in A–J and of DIAP1 and Hrb57A in K–T. Bar, 5 μm.

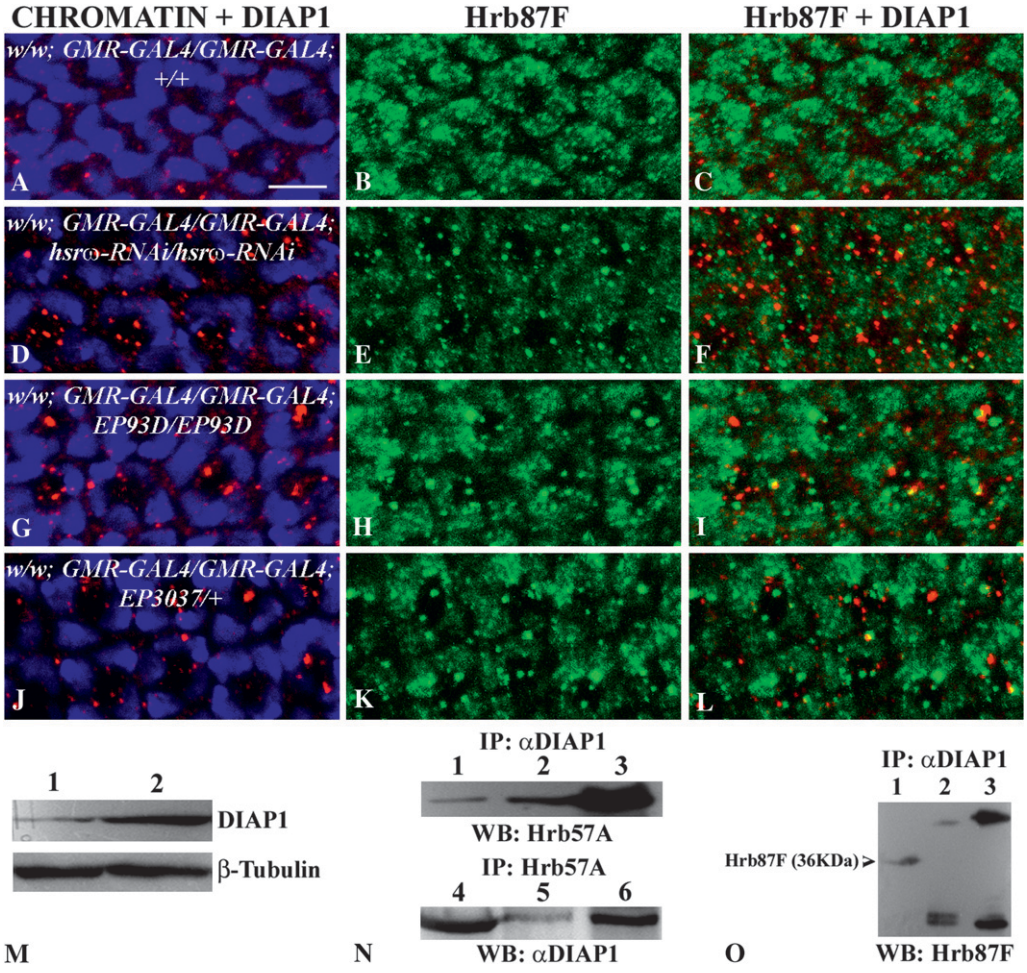

FIGURE 8.—DIAP1 does not colocalize with Hrb87F in larval eye discs. Projections of confocal images of late third instar larval eye discs are shown (genotype for each row is indicated in the first column) immunostained with anti-αDIAP1 (red, A, C, D, F, G, I, J, and L) and anti-Hrb87F (green, B, C, E, F, H, I, K, and L) and counterstained with DAPI (blue, A, D, G, and J). Merged images of DIAP1- and DAPI-stained nuclei are shown in A, D, G, and J and of DIAP1 and Hrb87F in C, F, I, and L. Bar, 5 μm. (M) Western blot showing increase in the level of DIAP1 in *GMR-GAL4/+; GMR-rpr/hsrω-RNAi* (lane 2) compared to that in *GMR-GAL4/+; GMR-rpr/+* (lane 1) adult heads; the bottom panel shows β-tubulin levels as a loading control. (N) Downregulation of hsrω transcripts increases association between DIAP1 and Hrb57A: the amount of Hrb57A immunoprecipitated with anti-αDIAP1 from wild-type third instar larval eye-imaginal discs (lane 1) is less than that from the *GMR-GAL4*-driven *hsrω-RNAi* (lane 2) discs. Likewise, immunoprecipitation with anti-Hrb57A pulls down a higher amount of DIAP1 from *GMR-GAL4/GMR-GAL4; hsrω-RNAi/hsrω-RNAi* (lane 6) than from *GMR-GAL4/GMR-GAL4; +/+* (lane 5) third instar larval eye discs. Lanes 3 and 4 show Hrb57A and DIAP1 proteins, respectively, in the crude extracts used for immunoprecipitation. (O) Immunoprecipitation with anti-αDIAP1 does not pull down Hrb87F either in wild type (lane 2) or in *GMR-GAL4/GMR-GAL4; hsrω-RNAi/hsrω-RNAi* (lane 3); the two bands in lanes 2 and 3 correspond to IgG heavy and light chains, respectively. Lane 1 shows the Hrb87F protein (arrowhead) in the crude extract of wild-type larval eye discs.

Figure 9, D and H, $N = 917$). Intriguingly, however, expression of the *EP93D* or *EP3037* alleles in an Eiger overexpression background did not increase the frequency of dying pupae (Table 3).

Transforming growth factor β (TGF-β)-activated kinase1 (TAK1), a component of the Drosophila JNK pathway, belongs to the MAPKKK superfamily that specifically activates the JNK pathway *in vivo* and mediates both cell shape and apoptotic responses in Drosophila (TAKATSU *et al.* 2000). The nonpigmented and small eye phenotype resulting from overexpression of *dTAK1* (Figure 9, I and M; $N = 469$) was also significantly suppressed by coexpression of *hsrω-RNAi* (Figure 9, J and N; $N = 1218$). On the other hand, augmentation of hsrω transcript levels through expression of *EP93D* or *EP3037* exaggerated the eye damage (Figure 9, K and O, $N = 241$; and Figure 9, L and P, $N = 266$, respectively).

GMR-GAL4-driven expression of *dTAK1* caused a major fraction of the progeny (44.8%, $N = 1047$) to die as differentiated pupae (Table 3). Downregulation of hsrω-n transcript levels with one copy of *hsrω-RNAi* facilitated emergence of a substantially greater proportion of *GMR-GAL4/UAS-dTAK1; hsrω-RNAi/+* pupae as adults (Table 3). However, an increase in the level of hsrω transcripts by *GMR-GAL4* driven coexpression of *EP93D* (42.2%, $N = 417$) or *EP3037* (47.7%, $N = 509$) in the *dTAK1* background did not significantly alter the proportion of progeny dying as differentiated pupae.

Tumor necrosis factor receptor-associated factors (TRAFs) are a family of intracellular adaptor proteins that transduce signals, including JNK activation (CHA *et al.* 2003). Eyes of adults carrying one copy each of both *GMR-GAL4* and *UAS-DTRAF1 (EP0578)* showed a rough eye surface (Figure 9Q; $N = 279$) with disorganized

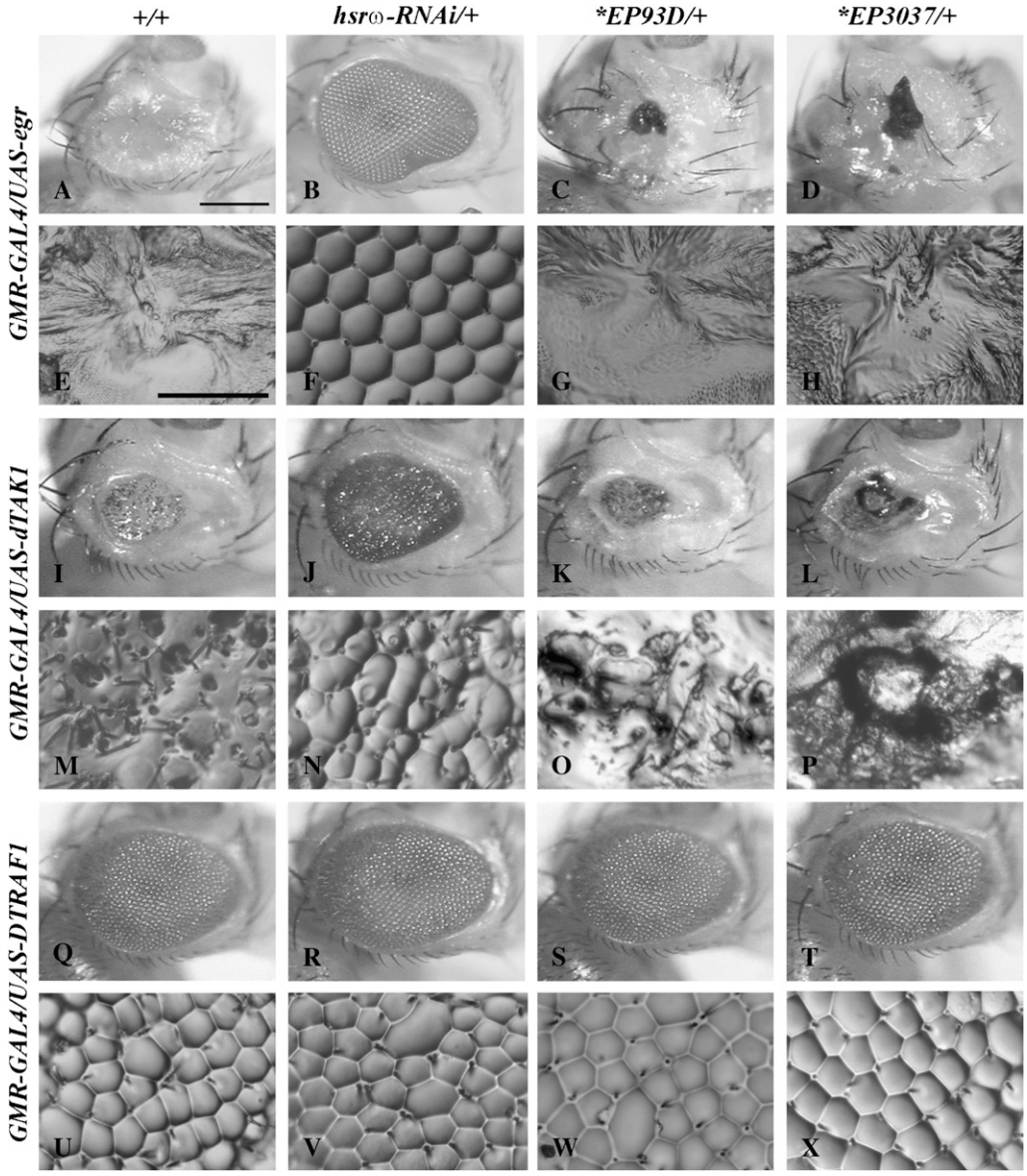

FIGURE 9.—Genetic interaction between *hsr*ω and the JNK signaling pathway components. *hsr*ω-*RNAi* effectively rescues JNK-mediated cell death. (A–D, I–L, and Q–T) Light micrograph images of adult eyes; (E–H, M–P, and U–X) nail polish imprints of the eye surface. Genotypes common to rows are indicated on the left while those for columns are indicated on top. Bars: for A–D, I–L, and Q–T in A and for E–H, M–P, and U–X in E, 20 μm.

arrays of ommatidia (Figure 9U). Surprisingly, eyes of adult flies coexpressing a single copy each of *hsr*ω-*RNAi* (Figure 9, R and V; $N = 292$) or *EP93D* (Figure 9, S and W; $N = 288$) or *EP3037* (Figure 9, T and X; $N = 267$) in the above background were indistinguishable from those of flies carrying single copies of *GMR-GAL4* and *UAS-DTRAF1* (Figure 9, Q and U). Thus, modulation of hsrω transcript levels does not appear to affect DTRAF1-induced apoptotic death.

The noncoding hsrω-n RNA is necessary for JNK activation during apoptosis: The *puckered* (*puc*) gene encodes a phosphatase that negatively regulates the activity of the JNK pathway (MARTIN-BLANCO *et al.* 1998). The *puc[E69]* allele, a P *lacZ* enhancer-trap line inserted in the *puc* gene (RING and MARTINEZ ARIAS 1993), results in the hyperactivation of JNK (MARTIN-BLANCO *et al.* 1998). Introduction of a single copy of *puc[E69]* dramatically enhanced the reduced eye phenotype of *GMR-GAL4/UAS-egr; +/+* flies (compare Figure 10, A and B, with Figure 9, A and E). The *GMR-GAL4/UAS-egr; puc[E69]/+* flies displayed a prominent black lesion in place of the eye (Figure 10, A and B; $N = 195$). However, coexpression of a single copy of *hsr*ω-*RNAi* strongly suppressed (Figure 10, E and F; $N = 218$) the severe eye degeneration in *GMR-GAL4/UAS-egr; puc[E69]/+* flies, restoring the ommatidial integrity and eye size to almost that of wild type (not shown).

JNK signaling in Drosophila is reflected in the expression levels of *puckered* since it is transcriptionally induced by *Basket* (dJNK) (MARTIN-BLANCO *et al.* 1998). To further validate the above results of genetic interaction studies, we examined if the JNK activity is modulated by levels of hsrω transcripts. The activity of JNK signaling *in vivo* was measured by the *puckered-LacZ* enhancer trap reporter assay. As expected, X-gal staining (Figure 10, C and G) or immunostaining with a

TABLE 3

Downregulation of the noncoding hsrω transcripts rescues JNK-mediated pupal lethality

Genotype	*N*	% dying as differentiated pupae
GMR-GAL4/UAS-egr; +/+	2590	36.2
GMR-GAL4/UAS-egr; hsrω-RNAi^{3}*/+*	1724	0.5
GMR-GAL4/UAS-egr; EP93D/+	1290	38.0
GMR-GAL4/UAS-egr; EP3037/+	1417	35.3
GMR-GAL4/UAS-dTAK1; +/+	1047	44.8
GMR-GAL4/UAS-dTAK1; hsrω-RNAi^{3}*/+*	1243	2.0
GMR-GAL4/UAS-dTAK1; EP93D/+	417	42.2
GMR-GAL4/UAS-dTAK1; EP3037/+	509	47.7

β-galactosidase antibody (Figure 10, D and H) revealed a strong induction of *puc-LacZ* (Figure 10, C and D, respectively) in the region posterior to the morphogenetic furrow in eye discs from *GMR-GAL4/UAS-egr; puc[E69]/+* third instar larvae. This staining was dramatically reduced in eye discs from *GMR-GAL4/UAS-egr; puc[E69]/hsrω-RNAi* larvae (Figure 10, G and H).

The extent of JNK phosphorylation in larval eye discs either expressing *GMR-GAL4*-driven *UAS-egr* alone or coexpressing both *UAS-egr* and the *hsrω-RNAi* or *UAS-egr* and the *EP3037* transgenes was assayed with a phospho-JNK-specific antibody. To examine the arrangement of photoreceptor cells, eye discs of the above genotypes were co-immunostained with the Elav antibody. As expected, JNK phosphorylation was clearly evident in the region of *egr* overexpression (Figure 11, A–C). In contrast, downregulation of hsrω-n RNA in an *egr* overexpression background dramatically reduced JNK activation as seen by near complete absence of the characteristic punctate staining (Figure 11, D–F). Increased expression of the *hsrω* gene in *GMR-GAL4/UAS-egr; EP3037/+* larval eye discs resulted in a slight upregulation of JNK activity in comparison to discs expressing *egr* alone (compare Figure 11B and 11H). Interestingly in these discs, the ommatidial arrays were highly disorganized as revealed by DAPI staining of photoreceptor nuclei (compare Figure 11A and 11G). Examination of Elav staining in *GMR-GAL4*-driven *UAS-egr*-expressing third instar eye discs revealed degeneration of photoreceptor nuclei (Figure 11C). Although Elav-stained photoreceptors appeared larger in the Eiger-expressing larval eye discs, the number and the compact arrangement of Elav positive cells were significantly reduced in these discs when compared to the *GMR-GAL4/UAS-egr; hsrω-RNAi/+* discs (compare Figure 11C and 11F). In contrast, *GMR-GAL4*-driven expression of *EP3037* in larval eye discs resulted in enhanced deterioration of photoreceptors as revealed by the highly abnormal shape and the loose arrangement of the developing ommatidial units accompanied by a prominent reduction in Elav staining in these cells (Figure 11I).

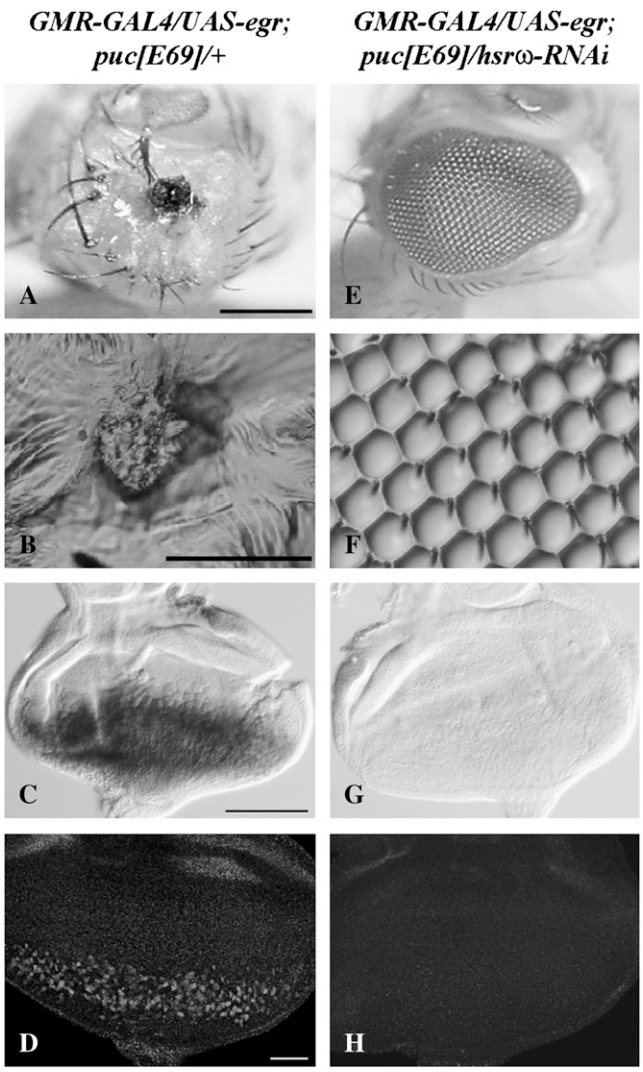

FIGURE 10.—Enhancement of *egr*-induced eye degeneration by reduced levels of Puc is ameliorated by depletion of hsrω transcripts. Photomicrographs (A and E) and nail polish imprints (B and F) of eyes of *GMR-GAL4/UAS-egr; puc*^{E69}*/+* (A and B) and *GMR-GAL4/UAS-egr; puc*^{E69}*/hsrω-RNAi* (E and F) flies are shown. C and G are DIC images of X-gal-stained eye discs and D and H are confocal projections of β-galactosidase antibody-stained eye discs from *GMR-GAL4/UAS-egr; puc*^{E69}*/+* (C and D) and *GMR-GAL4/UAS-egr; puc*^{E69}*/hsrω-RNAi* (G and H) third instar larvae, respectively, showing the β-galactosidase reporter activity. Bars: for A and E in A and B and F in B, 20 μm; for C and G in C, 100 μm; and for D and H in D, 50 μm.

Downregulation of hsrω transcripts fails to suppress *egr*-induced apoptosis in the presence of the DIAP1-RNAi transgene: Eiger induces DIAP1 sensitive cell death through the activation of the JNK signaling cascade in Drosophila (IGAKI *et al.* 2002). As reported earlier (IGAKI *et al.* 2002; MORENO *et al.* 2002), expression of *UAS-DIAP1* ($N = 219$) suppressed the Eiger-

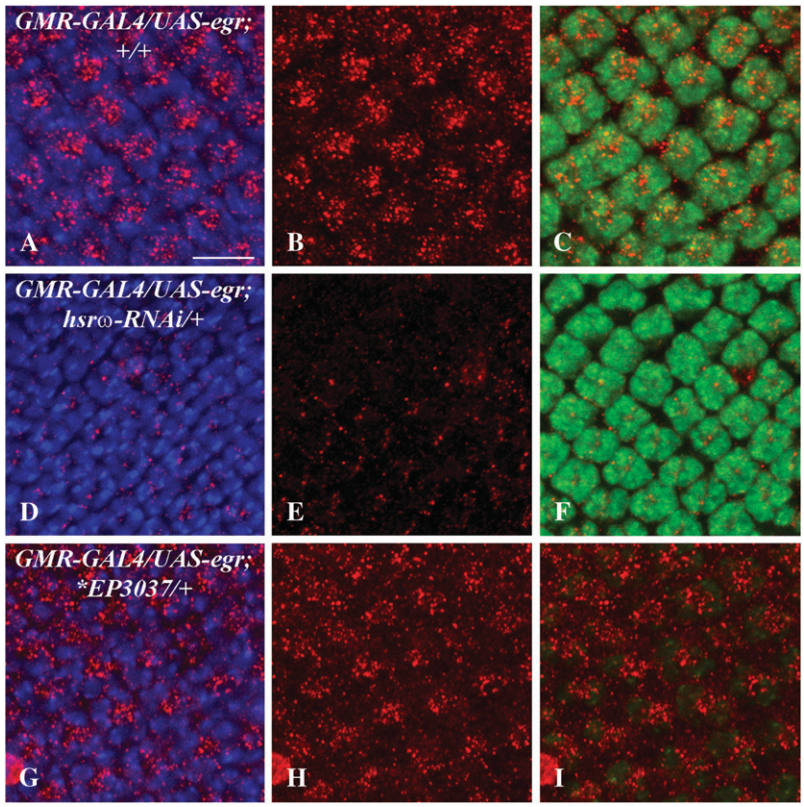

FIGURE 11.—Depletion of hsrω transcripts suppresses activation of the JNK signaling cascade in Drosophila eye discs. Shown are projections of confocal images of late third instar larval eye discs (genotypes for each row are indicated in the first column) immunostained with active JNK (red, B, E, and H) and elav (green, C, F, and I) antibodies and counterstained with DAPI (blue, A, D, and G). Merged images of active JNK and DAPI-stained nuclei are presented in A, D, and G and those of active JNK and Elav-stained photoreceptors are in C, F, and I. Bar, 10 μm.

induced eye ablation (compare Figure 12, A and E, with Figure 9, A and E), while RNAi-mediated depletion of DIAP1 enhanced the Eiger-mediated eye damage leading to the formation of black lesions in place of the eye (compare Figure 12, C and G, with Figure 9, A and E; N = 323). On the other hand, coexpression of both *UAS-DIAP1* and a single copy of the *hsrω-RNAi* transgene completely restored the eye morphology and size such that the eyes of *GMR-GAL4/UAS-egr; UAS-DIAP1/hsrω-RNAi* (Figure 12, B and F; N = 201) flies could not be distinguished from those of wild-type flies. Significantly, however, in the presence of the *DIAP1-RNAi* transgene, coexpression of one copy of *hsrω-RNAi* (Figure 12, D and H; N = 94) failed to rescue the Eiger-induced eye damage.

Depletion of hsrω transcripts inhibits Eiger-induced activation of effector caspases: Targeted overexpression of Eiger in the developing eye disc induces caspase-dependent apoptosis leading to severe ablation of the eye in adult flies (Figure 9, A and E). To determine the levels of active caspase-3 and to study organization of individual ommatidial cells soon after the onset of Eiger expression, eye discs of larvae expressing *GMR-GAL4*-driven *UAS-egr* in *hsrω-RNAi/+* (N = 9) and *EP3037/+* (N = 6) backgrounds were immunostained with the active caspase-3 and the mAb22C10 antibodies. As controls, eye discs from wild-type (N = 8) and *GMR-GAL4/UAS-egr; +/+* (N = 10) larvae were immunostained with these antibodies. Overexpression of Eiger led to increased active caspase-3 staining and disarrayed axonal projections in the optic stalk (Figure 13B; N = 10). In contrast, the ommatidia and axonal projections in *GMR-GAL4/UAS-egr; hsrω-RNAi/+* larval eye discs (N = 9) were organized as in wild type (compare Figure 13A and 13C); likewise, the staining for activated caspase-3 (Figure 13C) in *UAS-egr* and *hsrω-RNAi* coexpressing discs was nearly similar to that seen in wild type (Figure 13A). On the other hand, increased expression of hsrω transcripts using the *EP3037* allele caused severe disorganization of the ommatidial units and their projections with loss of individual ommatidial cellular integrity and irregular axonal connections to the optic stalk (Figure 13D). Similarly, the level of active caspase-3 in *GMR-GAL4/UAS-egr; EP3037/+* eye discs was considerably higher (Figure 13D; N = 6) than in eye discs expressing Eiger alone (Figure 13B).

Downregulation of hsrω transcript levels does not affect cell death mediated by overexpression of components of the EGFR signaling pathway in Drosophila: In the developing eye, tyrosine kinase signaling (mainly via the EGFR) is required to provide survival cues during photoreceptor differentiation (BERGMANN *et al.* 1998, 2002; FREEMAN 2002). EGFR signaling leads to activation of the Drosophila Ras homolog and protects cells against apoptosis. Eyes of adults carrying one copy each of both *GMR-GAL4* and a dominant-negative version of the EGF receptor (DER) were severely reduced in size (N = 239) and mostly devoid of the ommatidial organization (Figure 14, A and C). Ectopic expression of *argos*, a natural inhibitor of EGFR under control of

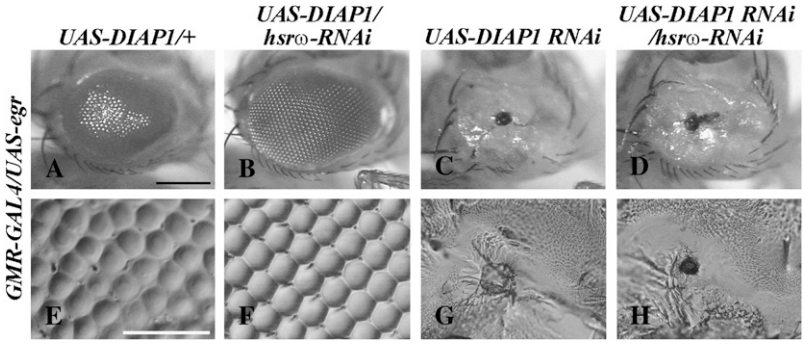

FIGURE 12.—Suppression of *egr*-induced cell death following depletion of hsrω transcripts is abrogated in the presence of the *DIAP1-RNAi* transgene. (A–D) Light micrographs of adult eyes; (E–H) nail polish imprints of the eye surface. Genotype common to the rows is indicated on the left while that for each column is indicated on the top. Bars: for A–D in A and E–H in E, 20 μm.

the eye-specific *GMR* promoter, caused roughening of the eye surface (Figure 14E; $N = 226$) with disorganization of ommatidial arrays (Figure 14G). Surprisingly, the eyes of adult flies coexpressing a single copy of *hsrω-RNAi* (Figure 14, B and D, $N = 218$; and Figure 14, F and H, $N = 203$) in the above backgrounds did not display any suppression of the cell death phenotypes observed following targeted overexpression of either DER or *argos*. Thus, modulation of hsrω transcript levels does not appear to affect EGFR-induced apoptotic death in the developing eye discs.

Induced cell death is suppressed by downregulation of hsrω-n transcripts in other appendages as well: To determine whether the hsrω transcripts affect induced cell death in adult appendages other than the eye in flies, we analyzed the effects of hsrω-n RNAi on apoptosis caused by ectopic expression of either *UAS-rpr* or *UAS-egr* in the developing wing. Ectopic expression of *egr* in the dorsoventral compartments of the developing wing discs under control of the *vg-GAL4* driver caused organ ablation leading to the formation of reduced and vestigial wings in adult flies (Figure 15A; $N = 194$). Likewise, *vg-GAL4*-mediated overexpression of *rpr* in the developing wing discs led to ablation of the alula and axillary cell (Figure 15C; $N = 180$). Downregulation of hsrω transcripts using a single copy of the *hsrω-RNAi* transgene in the above backgrounds restored the wing morphology (Figure 14, B and D) such that wings of *UAS-egr/+; hsrω-RNAi/vg-GAL4* (Figure 15B; $N = 212$) or *UAS-rpr/+; hsrω-RNAi/vg-GAL4* (Figure 14D; $N = 168$) could not be distinguished from those of wild-type flies.

In addition, it was seen that ectopic expression of Eiger in a *puc[E69]* background led to degeneration of the arista. A similar effect was also seen in an Eiger overexpression background following augmentation of hsrω transcript levels using any of the two *EP* alleles, *EP93D* or *EP3037* (not shown). However, the phenotype was completely suppressed by simultaneous expression of the *hsrω-RNAi* transgene in any of the above backgrounds (not shown). Thus, suppression of induced apoptosis following loss of hsrω transcripts is not limited to the eye but extends to other appendages also.

DISCUSSION

We show a novel regulatory role of the noncoding hsrω transcripts of *D. melanogaster* in apoptosis induced by ectopic expression of a variety of proapoptotic stimuli like the RHG proteins, initiator or effector caspases, and JNK signaling components. All these instances of induced apoptosis in the developing eye and

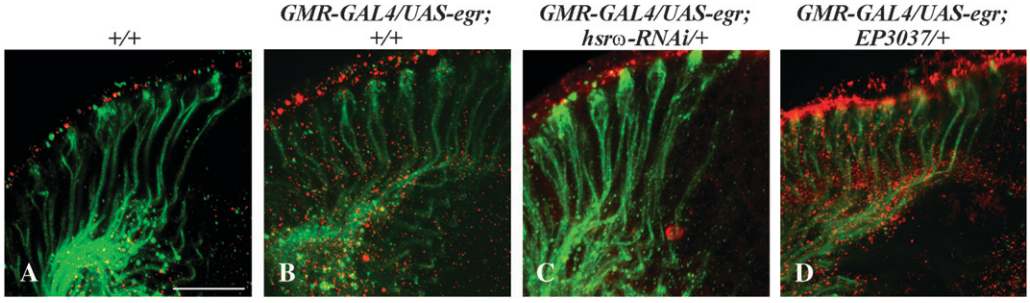

FIGURE 13.—Altered levels of hsrω transcripts modulate activated effector caspase activity in eye cells. (A–D) Projections of confocal images of late third instar larval eye discs coimmunostained with mAb22C10 (green, A–D) and Drosophila effector caspase DrICE (red, A–D) antibodies to show axonal projections from developing rhabdomeres (green) and active effector caspase (red) in +/+ (A), *GMR-GAL4/UAS-egr; +/+* (B), *GMR-GAL4/UAS-egr; hsrω-RNAi/+* (C), and *GMR-GAL4/UAS-egr; EP3037/+* (D). Bar, 20 μm.

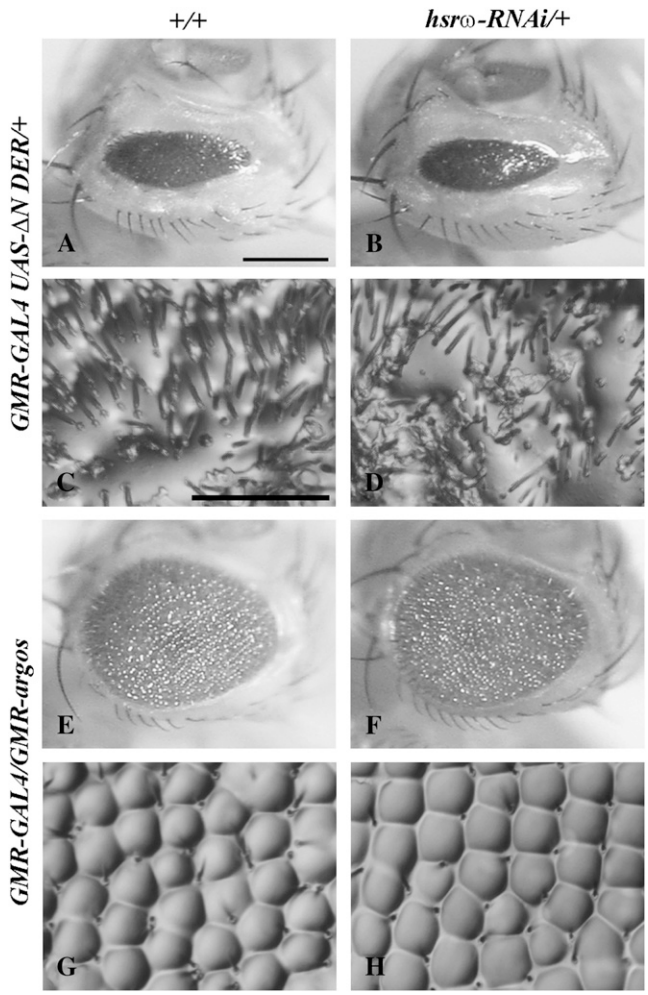

FIGURE 14.—Depletion of hsrω transcripts does not modify cell death phenotypes induced by ectopic overexpression of components of the EGF receptor (EGFR) signaling pathway. A, B, E, and F are photomicrographs and C, D, G, and H are nail polish imprints of adult eyes. Genotypes common to rows (chromosome 2) are indicated on the left while those for columns (chromosome 3) are indicated on top. Bars: for A, B, E, and F in A and C, D, G, and H in C, 20 μm.

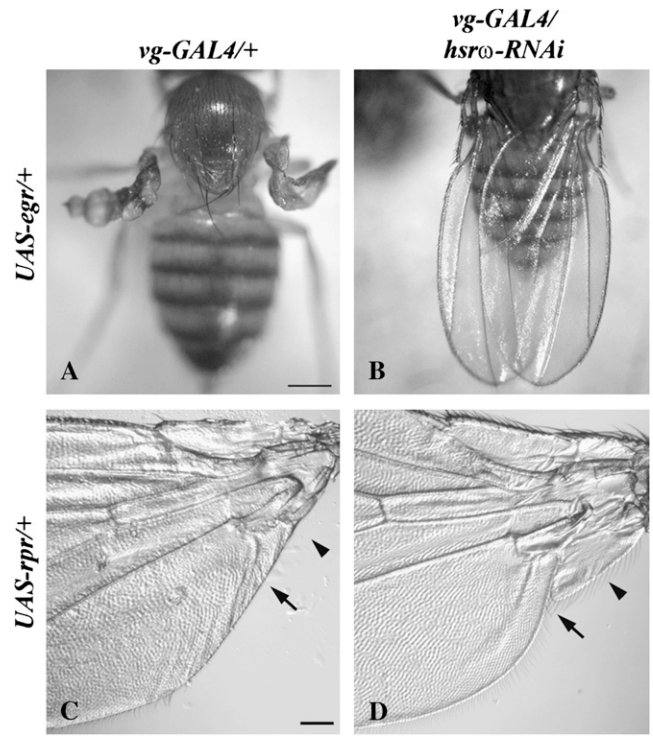

FIGURE 15.—Depletion of hsrω-n RNA effectively ameliorates cell death phenotypes in the developing wing. Targeted expression of *egr* (A) in the wing causes organ ablation, which is completely blocked (B) by downregulation of the hsrω-n transcripts. Expression of *UAS-rpr* with *vg-GAL4* (C) causes ablation of the alula (arrowhead) and the axillary cell (arrow) in fly wings, but *vg-GAL4*-driven coexpression of the *hsrω-RNAi* and *UAS-rpr* (D) transgenes in wing discs prevents their ablation. Bars: for A and B in A, 20 μm; and for C and D in C, 100 μm.

other imaginal discs were dominantly suppressed by depletion of hsrω transcripts but enhanced by overexpression of this noncoding gene.

Our results suggest that reduced cellular levels of hsrω transcripts inhibit induced apoptosis through multiple paths, *i.e.*, (i) by preventing activation of procaspases, (ii) by inhibiting activity of the effector caspases, and (iii) by suppressing activation of JNK signaling. While the first two paths seem to be mediated via DIAP1, the downregulation of JNK signaling by hsrω-RNAi may involve, besides DIAP1, other mediator(s) as well.

Diverse death signals in Drosophila cells upregulate Rpr, Hid, and Grim (RHG) proteins, which release the initiator and effector caspases from the inhibitory association with DIAP1, thereby resulting in apoptosis by the activated caspases (VERNOOY *et al.* 2000). In addition to inhibiting the binding of DIAP1 with initiator and effector caspases, the RHG proteins also greatly decrease DIAP1 abundance through multiple pathways, some of which are regulated in a tissue-specific manner (HAYS *et al.* 2002; YOO *et al.* 2002). Besides enhancing ubiquitin-mediated degradation of DIAP1, Rpr and Grim also suppress global protein translation, which results in relatively greater levels of free Dronc since the half-life of DIAP1 is shorter than that of Dronc (HOLLEY *et al.* 2002; YOO *et al.* 2002). We observed that while *hsrω-RNAi* expression substantially suppressed Rpr- and Grim-induced apoptosis, that induced by ectopic expression of Hid in eye discs was not much affected. This seems to be related to differences in some of the pathways followed by the different RHG proteins in inducing apoptosis. Ectopic expression of Hid triggers apoptosis in eye disc cells but this is not associated with reduction in cellular levels of DIAP1 as happens following Rpr or Grim expression (HAYS *et al.* 2002). This suggests that the Hid pathway probably releases the initiator and effector caspases from the inhibitory action of DIAP1 without its degradation. Apparently, the hsrω transcripts do not modulate this alternative

path used by Hid to bring about activation of caspases. Further, while EGFR inhibits Hid-mediated apoptotic activity in cells that are destined to survive, it has no effect on Rpr- and Grim-induced cell death (Bergmann *et al.* 1998; Kurada and White 1998). These differences in the pro-apoptotic actions of Hid on one hand and Rpr and Grim on the other also seem to provide a basis for our finding that apoptosis following overexpression of components of the EGFR signaling pathway is not affected by varying levels of hsrω transcripts.

Caspases are synthesized as zymogens and are activated by proteolysis upon pro-apoptotic signaling. We show that downregulation of hsrω transcripts not only blocks induced cell death by inhibiting activation of the "effector" or executioner caspases (active caspase-3, Figure 4) by the apical or "initiator" caspases (such as Dronc, Figure 4) but also prevents downstream actions of even the active effector caspases. Our immunostaining and Western blotting results clearly show that depletion of hsrω transcripts elevates the cellular levels of DIAP1, which acts as a central brake on the apoptotic cascade (reviewed by Hay 2000). That DIAP1 is the major target through which hsrω-RNAi inhibits apoptosis is also indicated by its failure to suppress apoptosis induced by Rpr or Grim or Eiger in the DIAP1-RNAi background (Figures 6 and 12).

The observation that the DIAP1-RNAi-induced eye phenotype or pupal lethality was much less in the w^+ than in the *w* background is intriguing. This raises the possibility that presence of the w^+ allele affects DIAP1-RNAi-induced cell death and consequently the improved eye phenotype following coexpression of the different *hsrω-RNAi* transgenes may be due to additional copies of the *mini-white* marker rather than to suppression of cell death following hsrω-RNAi. In this context, it should be noted that many of the transgenic lines used in our present and other studies also carry the same *mini-white* marker with equally varying levels of eye pigment expression but they do not by themselves provide recovery from the eye degeneration as does expression of the *hsrω-RNAi* transgene; the undriven *hsrω-RNAi* transgene, which expresses the *mini-white* marker, also by itself does not suppress induced apoptosis. Furthermore, the EP transposons present in *EP93D* or *EP3037* also carry the *mini-white* marker, yet expression of any of these alleles worsens the DIAP1-RNAi eye phenotype. Likewise, flies of the genotype *w/w; GMR-GAL4 UAS-DIAP1-RNAi/+; GMR-rpr/hsrω-RNAi* carrying four copies of the *mini-white* marker still show degenerated eyes. Therefore, recovery in eye phenotype seen following coexpression of the *DIAP1-RNAi* and the *hsrω-RNAi* transgenes is due to the reduced levels of hsrω transcripts. Significantly less damage brought about by DIAP1-RNAi in the presence of the w^+ allele on the X chromosome compared to that in the X-chromosomal *w* background may be related to our finding that the DIAP1 level in *w/w* eye disc cells was less than that seen in the wild-type discs. Reasons for this difference remain to be analyzed.

Although the *GMR* promoter is generally believed to be specifically active only in eye cells, we found that *GMR-GAL4*-driven expression of various mutant forms of Dronc, DIAP1-RNAi, Eiger, or dTAK1 resulted in varying degrees of pupal lethality presumably due to leaky or otherwise expression in certain other cells whose activity is vital for survival of the organism. Notwithstanding the nature of these cells and the damage, it is interesting in the present context that *hsrω-RNAi* substantially suppressed such lethality while overexpression of these transcripts generally elevated it. This suggests that the hsrω transcript levels have comparable effects on perturbations that follow the ectopic activation of the apoptotic cascade in eye as well as other cell types in which the *GMR-GAL4* driver causes the target gene(s) to express. An intriguing observation during this study was that the suppression of *GMR-GAL4*-driven Dronc-induced pupal lethality (Table 1) by coexpression of the *hsrω-RNAi* transgene was greater for females than for males. Though the basis of this sex-specific effect is not known, it may be related to the role of hsrω transcripts in metabolism of a variety of RNA-binding proteins, including Sxl (Lakhotia *et al.* 1999; Prasanth *et al.* 2000; Jolly and Lakhotia 2006). This needs to be examined further.

Our results clearly show that depletion of hsrω transcripts through RNAi elevates the DIAP1 levels in cells in which apoptosis is induced either by homozygosity of the *GMR-GAL4* driver or because of the targeted expression of Rpr. Our results also provide an interesting insight into how the noncoding nuclear hsrω transcripts stabilize DIAP1 in cells induced to undergo apoptosis. As reported earlier (Lakhotia *et al.* 1999; Prasanth *et al.* 2000; Jolly and Lakhotia 2006), the hsrω-n transcripts specifically associate with a variety of nuclear hnRNPs and other related RNA-processing proteins to form fine nucleoplasmic omega speckles that regulate the availability of these proteins. Our present results show for the first time that DIAP1 interacts with Hrb57A, since not only do their distributions partially overlap with each other but also immunoprecipitation pulls down these proteins together, more so following hsrω-RNAi. Downregulation of hsrω transcripts is associated with disappearance of the nucleoplasmic omega speckles (Mallik and Lakhotia 2009 and our present observations). Some of the hnRNPs and other RNA-binding proteins that are released from their sequestered state in the omega speckles now get redistributed. Much of the Hrb57A in eye disc cells expressing the *hsrω-RNAi* transgene moves to the cytoplasm where it associates with DIAP1. We believe that the enhanced association of Hrb57A with DIAP1 following hsrω-RNAi not only prevents the degradation of DIAP1 that otherwise happens in cells triggered to enter apoptosis but also blocks activation of initiator and effector caspases.

The finding that enhanced damage to eyes occurred following coexpression of *EP93D* or *EP3037* in Rpr-expressing cells (Figure 3) in spite of the high cellular levels of DIAP1 (Figure 7) was rather unexpected. This appears more intriguing in the context of the above-noted correlation between suppression of induced apoptosis and elevation of DIAP1 levels following hsrω-RNAi. It is known that DIAP1 has nonapoptotic roles as well (Hay *et al.* 2004) and likewise, the hsrω transcripts function as hubs in a variety of cellular networks by virtue of their interaction with several different classes of cellular proteins (Jolly and Lakhotia 2006; Arya *et al.* 2007). Consequently, alterations in cellular levels of the hsrω transcripts may have varied consequences depending upon specific cell physiology. In another study (M. Mallik and S. C. Lakhotia, unpublished results), we have shown that overexpression of *hsr*ω compromises proteasomal activity. Thus it is possible that while Rpr expression causes ubiquitination of DIAP1 for degradation (Holley *et al.* 2002), the ubiquitinated DIAP1 is not degraded because of the compromised ubiquitin–proteasome pathway in *EP3037*-expressing cells (M. Mallik and S. C. Lakhotia, unpublished results). This would result in the apparent greater accumulation of DIAP1 in cells with high levels of the hsrω transcripts although being ubiquitinated, it fails to suppress caspase activity. Another possibility is that the differences in redistribution of Hrb57A in eye disc cells expressing either *EP3037* or *hsrω-RNAi* affect the DIAP1 activity differently so that although in both case the DIAP1 is abundant, in *EP*-expressing cells it fails to inhibit the activation of caspases as is also known in the case of *GMR-hid*-mediated apoptotic cell death (Hays *et al.* 2002).

In normal eye disc and other cells, the Hrb87F protein (hnRNP A1 homolog) also associates with the hsrω transcripts in the nucleoplasmic omega speckles (Lakhotia *et al.* 1999; Prasanth *et al.* 2000) and, like Hrb57A, shows an altered distribution following depletion or overexpression of these noncoding transcripts (Mallik and Lakhotia 2009 and our present observations). However, Hrb87F does not associate with DIAP1 in the same manner as Hrb57A does following either up- or downregulation of hsrω transcript levels. Therefore, we believe that the regulation of cellular distribution of Hrb57A by the hsrω transcripts is more critical in the effects of these transcripts on induced apoptosis.

As noted above, Rpr and Grim inhibit global protein synthesis so that the short-lived DIAP1 polypeptides are turned over faster than those of Dronc and this initiates the apoptotic cascade (Holley *et al.* 2002). In this context, it is interesting to note that under conditions of global inhibition of cellular protein synthesis, the level of the small cytoplasmic hsrω-c transcript is enhanced (Bendena *et al.* 1989). It has also been reported more recently that the quantity and quality of hsrω transcripts affect levels of protein synthesis in flies (Johnson *et al.* 2009). Such possible effects of hsrω transcripts on the cellular translation apparatus may be yet another mechanism that may modulate cellular levels of DIAP1 in Rpr- or Grim-expressing cells. This interesting possibility needs further analysis.

JNK activation is one of the cellular responses that protect cells under stress. However, under acute stress, JNK activation can induce the cell death program (Kanda and Miura 2004). Our results show that altered levels of the noncoding hsrω transcripts affect JNK activation and thus modulate JNK-mediated apoptosis in Drosophila eye discs. Rpr-induced degradation of DIAP1 also modulates activation of the JNK pathway (Kanda and Miura 2004) since in the presence of Rpr, DIAP1 undergoes self-ubiquitination and is degraded by the proteasome and the consequent stabilization of DTRAF1 activates JNK-mediated cell death (Holley *et al.* 2002; Kuranaga *et al.* 2002; Kanda and Miura 2004). It is likely that the observed inhibition of JNK activation following hsrω-RNAi results from degradation of DTRAF1 due to elevation of the endogenous DIAP1 levels in these cells. This finds support in our observation that altered levels of *hsr*ω transcripts did not modify the rough eye phenotype resulting from overexpression of DTRAF1. Apparently, the enhanced DIAP1 levels following expression of the *hsrω-RNAi*, the *EP3037*, or the *EP93D* transgenes are not sufficient to counteract the concomitant increase in DTRAF1 levels such that excess DTRAF1 can still activate the JNK pathway to induce caspase-mediated cell death.

It has been reported earlier (Moreno *et al.* 2002) that Eiger-induced apoptotic death is presumably mediated through Hid because the Eiger overexpressing eye disc cells show a strong transcriptional activation of *hid*. In view of this, our present finding that hsrω-RNAi robustly suppresses Eiger-induced cell death (Figure 9) but fails to modulate Hid-induced apoptosis (Figure 3) appears unusual. While it remains possible that Eiger brings about apoptosis in a Hid-independent manner that is sensitive to hsrω transcript levels, our observations on suppression of Eiger-mediated JNK activation by hsrω-RNAi provide a plausible explanation as to why Eiger- but not Hid-induced cell death is inhibited by hsrω-RNAi. It is known that JNK activation is sufficient to induce Hid (Luo *et al.* 2007) and that Eiger induces cell death by activating the Drosophila JNK pathway (Igaki *et al.* 2002; Moreno *et al.* 2002). Thus it is likely that the Eiger-induced upregulation of *hid* is mediated through activation of JNK. Our observations show that hsrω-RNAi suppresses the Eiger-induced activation of JNK. Consequently, in spite of Eiger overexpression, *hid* is not upregulated and, therefore, apoptosis does not occur.

Recent work in our laboratory (Arya and Lakhotia 2008) demonstrated that depletion of Hsp60D, one of the Hsp60 family proteins in Drosophila, also suppressed induced apoptosis. It was suggested that RNAi-mediated downregulation of Hsp60D transcripts rescued induced

cell death phenotypes because dissociation of DIAP1 from initiator and executioner caspase complexes requires the Hsp60D protein (Arya and Lakhotia 2008). It is interesting that although Hsp60D as well as the noncoding hsrω transcripts seem to be preventing induced apoptosis largely via the DIAP1, there are some notable differences in their mechanisms. For instance, downregulation of Hsp60D ameliorated the *GMR-hid*-mediated reduced eye phenotype (Arya and Lakhotia 2008) to a greater extent than that seen following expression of the *hsrω-RNAi* transgene. In addition, while depletion of Hsp60D blocked apoptosis triggered by JNK as well as EGFR signaling, reduction in hsrω-n transcript levels modulated apoptotic death triggered by activation of the JNK pathway but not that following EGFR signaling. Further studies are required to understand the specific interaction(s) between hsrω transcripts, Hsp60D, and DIAP1.

It is interesting that global expression of the *hsrω-RNAi* transgene, *e.g.*, under the *Act5C-GAL4* driver, results in a high incidence of organismic lethality (M. Mallik and S. C. Lakhotia, unpublished results) but this is unlikely to be due only to inhibition of developmental apoptosis since the survivors are phenotypically normal. We believe that, like the multiple regulatory roles of the miRNAs (Alvarez-Garcia and Miska 2005), large noncoding RNAs like the hsrω transcripts have multiplexing roles in cells because of their capacity to bind/associate with diverse proteins. As is being increasingly realized, the same or related proteins participate in different cellular pathways and therefore any perturbations in them can have diverse functional consequences depending upon the state of cellular protein and RNA networks (Promislow 2004; He and Zhang 2006). Consequently, altered levels of the hsrω transcripts can be expected to have very different outcomes depending upon the specific physiological state of the cell. This is indeed the case since while hsrω-RNAi suppresses neurodegeneration in eye discs that express proteins with expanded poly(Q) stretches (Mallik and Lakhotia 2009), cells with reduced amounts of hsrω transcripts die following otherwise nonlethal heat shock (our unpublished results). On the other hand, the present results show that hsrω-RNAi suppresses induced apoptosis.

Our study provides the first example of a constitutively expressed and stress-inducible large noncoding RNA that modulates induced apoptosis in Drosophila. This adds a new dimension to the already known complex regulation of cell death (Arya *et al.* 2007). At the same time, this study further strengthens the view that some large noncoding RNAs act as hubs in cellular regulatory networks (Arya *et al.* 2007) and thus perform multiple roles in maintaining cellular homeostasis (Mallik and Lakhotia 2007; Mattick 2009).

We gratefully thank I. Muro, B. Hay, P. Meier, F. Leulier, M. Miura, J. Chung, M. Freeman, and the Bloomington Stock Center for providing the different fly stocks used in this study. We acknowledge Harold Saumweber for generously providing the P11 and Q18 antibodies and Kristin White for the DIAP1 antibody. This work was supported by a research grant from the Department of Science and Technology (DST), Government of India, New Delhi, to S.C.L. The Laser Scanning Confocal Microscopy Facility is also supported by the DST. M.M. is supported by the Shyama Prasad Mukherjee fellowship from the Council of Scientific and Industrial Research, New Delhi.

LITERATURE CITED

Akanksha, M. Mallik, R. Fatima and S. C. Lakhotia, 2008 The hsromega(05241) allele of the noncoding hsromega gene of *Drosophila melanogaster* is not responsible for male sterility as reported earlier. J. Genet. **87:** 87–90.

Alvarez-Garcia, I., and E. A. Miska, 2005 MicroRNA functions in animal development and human disease. Development **132:** 4653–4662.

Arya, R., and S. C. Lakhotia, 2006 A simple nail polish imprint technique for examination of external morphology of Drosophila eyes. Curr. Sci. **90:** 1179–1180.

Arya, R., and S. C. Lakhotia, 2008 Hsp60D is essential for caspase-mediated induced apoptosis in *Drosophila melanogaster*. Cell Stress Chaperones **13:** 509–526.

Arya, R., M. Mallik and S. C. Lakhotia, 2007 Heat shock genes—integrating cell survival and death. J. Biosci. **32:** 595–610.

Bendena, W. G., J. C. Garbe, K. L. Traverse, S. C. Lakhotia and M. L. Pardue, 1989 Multiple inducers of the Drosophila heat shock locus 93D (hsr omega): inducer-specific patterns of the three transcripts. J. Cell Biol. **108:** 2017–2028.

Bergmann, A., J. Agapite, K. McCall and H. Steller, 1998 The Drosophila gene hid is a direct molecular target of Ras-dependent survival signaling. Cell **95:** 331–341.

Bergmann, A., M. Tugentman, B. Z. Shilo and H. Steller, 2002 Regulation of cell number by MAPK-dependent control of apoptosis: a mechanism for trophic survival signaling. Dev. Cell **2:** 159–170.

Brand, A. H., and N. Perrimon, 1993 Targeted gene expression as a means of altering cell fates and generating dominant phenotypes. Development **118:** 401–415.

Cha, G. H., K. S. Cho, J. H. Lee, M. Kim, E. Kim *et al.*, 2003 Discrete functions of TRAF1 and TRAF2 in Drosophila melanogaster mediated by c-Jun N-terminal kinase and NF-kappaB-dependent signaling pathways. Mol. Cell. Biol. **23:** 7982–7991.

Chai, J., N. Yan, J. R. Huh, J. W. Wu, W. Li *et al.*, 2003 Molecular mechanism of Reaper-Grim-Hid-mediated suppression of DIAP1-dependent Dronc ubiquitination. Nat. Struct. Biol. **10:** 892–898.

Charroux, B., C. Angelats, L. Fasano, S. Kerridge and C. Vola, 1999 The levels of the bancal product, a Drosophila homologue of vertebrate hnRNP K protein, affect cell proliferation and apoptosis in imaginal disc cells. Mol. Cell. Biol. **19:** 7846–7856.

Evert, B. O., U. Wullner and T. Klockgether, 2000 Cell death in polyglutamine diseases. Cell Tissue Res. **301:** 189–204.

Freeman, M., 1996 Reiterative use of the EGF receptor triggers differentiation of all cell types in the Drosophila eye. Cell **87:** 651–660.

Freeman, M., 2002 A fly's eye view of EGF receptor signalling. EMBO J. **21:** 6635–6642.

Goyal, L., K. McCall, J. Agapite, E. Hartwieg and H. Steller, 2000 Induction of apoptosis by Drosophila reaper, hid and grim through inhibition of IAP function. EMBO J. **19:** 589–597.

Grether, M. E., J. M. Abrams, J. Agapite, K. White and H. Steller, 1995 The head involution defective gene of Drosophila melanogaster functions in programmed cell death. Genes Dev. **9:** 1694–1708.

Gunawardena, S., L. S. Her, R. G. Brusch, R. A. Laymon, I. R. Niesman *et al.*, 2003 Disruption of axonal transport by loss of huntingtin or expression of pathogenic polyQ proteins in Drosophila. Neuron **40:** 25–40.

Hawkins, C. J., S. L. Wang and B. A. Hay, 1999 A cloning method to identify caspases and their regulators in yeast: identification of Drosophila IAP1 as an inhibitor of the Drosophila caspase DCP-1. Proc. Natl. Acad. Sci. USA **96:** 2885–2890.

Hawkins, C. J., S. J. Yoo, E. P. Peterson, S. L. Wang, S. Y. Vernooy *et al.*, 2000 The Drosophila caspase DRONC cleaves following glutamate or aspartate and is regulated by DIAP1, HID, and GRIM. J. Biol. Chem. **275:** 27084–27093.

Hay, B. A., 2000 Understanding IAP function and regulation: a view from Drosophila. Cell Death Differ. **7:** 1045–1056.

Hay, B. A., and M. Guo, 2006 Caspase-dependent cell death in Drosophila. Annu. Rev. Cell. Dev. Biol. **22:** 623–650.

Hay, B. A., T. Wolff and G. M. Rubin, 1994 Expression of baculovirus P35 prevents cell death in Drosophila. Development **120:** 2121–2129.

Hay, B. A., D. A. Wassarman and G. M. Rubin, 1995 Drosophila homologs of baculovirus inhibitor of apoptosis proteins function to block cell death. Cell **83:** 1253–1262.

Hay, B. A., J. R. Huh and M. Guo, 2004 The genetics of cell death: approaches, insights and opportunities in Drosophila. Nat. Rev. Genet. **5:** 911–922.

Haynes, S. R., D. Johnson, G. Raychaudhuri and A. L. Beyer, 1991 The Drosophila Hrb87F gene encodes a new member of the A and B hnRNP protein group. Nucleic Acids Res. **19:** 25–31.

Hays, R., L. Wickline and R. Cagan, 2002 Morgue mediates apoptosis in the Drosophila melanogaster retina by promoting degradation of DIAP1. Nat. Cell Biol. **4:** 425–431.

He, X., and J. Zhang, 2006 Toward a molecular understanding of pleiotropy. Genetics **173:** 1885–1891.

Holley, C. L., M. R. Olson, D. A. Colon-Ramos and S. Kornbluth, 2002 Reaper eliminates IAP proteins through stimulated IAP degradation and generalized translational inhibition. Nat. Cell Biol. **4:** 439–444.

Igaki, T., H. Kanda, Y. Yamamoto-Goto, H. Kanuka, E. Kuranaga *et al.*, 2002 Eiger, a TNF superfamily ligand that triggers the Drosophila JNK pathway. EMBO J. **21:** 3009–3018.

Johnson, T. K., L. B. Carrington, R. J. Hallas and S. W. McKechnie, 2009 Protein synthesis rates in Drosophila associate with levels of the hsr-omega nuclear transcript. Cell Stress Chaperones (in press).

Jolly, C., and S. C. Lakhotia, 2006 Human sat III and Drosophila hsr omega transcripts: a common paradigm for regulation of nuclear RNA processing in stressed cells. Nucleic Acids Res. **34:** 5508–5514.

Kanda, H., and M. Miura, 2004 Regulatory roles of JNK in programmed cell death. J. Biochem. **136:** 1–6.

Kramer, J. M., and B. E. Staveley, 2003 GAL4 causes developmental defects and apoptosis when expressed in the developing eye of Drosophila melanogaster. Genet. Mol. Res. **2:** 43–47.

Kurada, P., and K. White, 1998 Ras promotes cell survival in Drosophila by downregulating hid expression. Cell **95:** 319–329.

Kuranaga, E., H. Kanuka, T. Igaki, K. Sawamoto, H. Ichijo *et al.*, 2002 Reaper-mediated inhibition of DIAP1-induced DTRAF1 degradation results in activation of JNK in Drosophila. Nat. Cell Biol. **4:** 705–710.

Kyriakis, J. M., and J. Avruch, 2001 Mammalian mitogen-activated protein kinase signal transduction pathways activated by stress and inflammation. Physiol. Rev. **81:** 807–869.

Lakhotia, S. C., 2003 The noncoding developmentally active and stress inducible hsr gene of Drosophila melanogaster integrates post-transcriptional processing of other nuclear transcripts, pp. 203–221 in *Noncoding RNAs: Molecular Biology and Molecular Medicine*, edited by J. Barciszewski and V. A. Erdmann. Kluwer Academic/Plenum, New York.

Lakhotia, S. C., and A. K. Singh, 1982 Non-inducibility of the 93D heat-shock puff in cold-reared larvae of *Drosophila melanogaster*. Chromosoma **92:** 48–54.

Lakhotia, S. C., P. Ray, T. K. Rajendra and K. V. Prasanth, 1999 The non-coding transcripts of hsr-omega gene in *Drosophila*: Do they regulate trafficking and availability of nuclear RNA-processing factors? Curr. Sci. **77:** 553–563.

Lakhotia, S. C., T. K. Rajendra and K. V. Prasanth, 2001 Developmental regulation and complex organization of the promoter of the non-coding hsr(omega) gene of Drosophila melanogaster. J. Biosci. **26:** 25–38.

Lee, C. Y., and E. H. Baehrecke, 2001 Steroid regulation of autophagic programmed cell death during development. Development **128:** 1443–1455.

Leulier, F., P. S. Ribeiro, E. Palmer, T. Tenev, K. Takahashi *et al.*, 2006 Systematic in vivo RNAi analysis of putative components of the Drosophila cell death machinery. Cell Death Differ. **13:** 1663–1674.

Lisi, S., I. Mazzon and K. White, 2000 Diverse domains of THREAD/DIAP1 are required to inhibit apoptosis induced by REAPER and HID in Drosophila. Genetics **154:** 669–678.

Luo, X., O. Puig, J. Hyun, D. Bohmann and H. Jasper, 2007 Foxo and Fos regulate the decision between cell death and survival in response to UV irradiation. EMBO J. **26:** 380–390.

Mallik, M., and S. C. Lakhotia, 2007 Non-coding DNA is not "junk" but a necessity for origin and evolution of biological complexity. Proc. Natl. Acad. Sci. India **77:** 43–50.

Mallik, M., and S. C. Lakhotia, 2009 RNAi for the large non-coding hsrω transcripts suppresses polyglutamine pathogenesis in Drosophila models. RNA Biol. (in press).

Martin-Blanco, E., A. Gampel, J. Ring, K. Virdee, N. Kirov *et al.*, 1998 puckered encodes a phosphatase that mediates a feedback loop regulating JNK activity during dorsal closure in Drosophila. Genes Dev. **12:** 557–570.

Mattick, J. S., 2009 The genetic signatures of noncoding RNAs. PLoS Genet. **5:** e1000459.

Meier, P., J. Silke, S. J. Leevers and G. I. Evan, 2000 The Drosophila caspase DRONC is regulated by DIAP1. EMBO J. **19:** 598–611.

Moreno, E., M. Yan and K. Basler, 2002 Evolution of TNF signaling mechanisms: JNK-dependent apoptosis triggered by Eiger, the Drosophila homolog of the TNF superfamily. Curr. Biol. **12:** 1263–1268.

Mutsuddi, M., and S. C. Lakhotia, 1995 Spatial expression of the hsr-omega (93D) gene in different tissues of Drosophila melanogaster and identification of promoter elements controlling its developmental expression. Dev. Genet. **17:** 303–311.

Prasanth, K. V., T. K. Rajendra, A. K. Lal and S. C. Lakhotia, 2000 Omega speckles—a novel class of nuclear speckles containing hnRNPs associated with noncoding hsr-omega RNA in Drosophila. J. Cell Sci. **113:** 3485–3497.

Promislow, D. E., 2004 Protein networks, pleiotropy and the evolution of senescence. Proc. Biol. Sci. **271:** 1225–1234.

Ray, P., and S. C. Lakhotia, 1998 Interaction of the non-protein-coding and stress-inducible hsrw gene with *Ras* genes of *Drosophila melanogaster*. J. Biosci. **4:** 377–386.

Riedl, S. J., and Y. Shi, 2004 Molecular mechanisms of caspase regulation during apoptosis. Nat. Rev. Mol. Cell. Biol. **5:** 897–907.

Ring, J. M., and A. Martinez Arias, 1993 puckered, a gene involved in position-specific cell differentiation in the dorsal epidermis of the Drosophila larva. Development (Suppl.): 251–259.

Sanchez, I., C. J. Xu, P. Juo, A. Kakizaka, J. Blenis *et al.*, 1999 Caspase-8 is required for cell death induced by expanded polyglutamine repeats. Neuron **22:** 623–633.

Saumweber, H., P. Symmons, R. Kabisch, H. Will and F. Bonhoeffer, 1980 Monoclonal antibodies against chromosomal proteins of Drosophila melanogaster: establishment of antibody producing cell lines and partial characterization of corresponding antigens. Chromosoma **80:** 253–275.

Sawamoto, K., A. Taguchi, Y. Hirota, C. Yamada, M. H. Jin *et al.*, 1998 Argos induces programmed cell death in the developing Drosophila eye by inhibition of the Ras pathway. Cell Death Differ. **5:** 262–270.

Sengupta, S., and S. C. Lakhotia, 2006 Altered expressions of the noncoding hsromega gene enhances poly-Q-induced neurotoxicity in Drosophila. RNA Biol. **3:** 28–35.

Song, Z., B. Guan, A. Bergman, D. W. Nicholson, N. A. Thornberry *et al.*, 2000 Biochemical and genetic interactions between Drosophila caspases and the proapoptotic genes rpr, hid, and grim. Mol. Cell. Biol. **20:** 2907–2914.

Spreij, T. E., 1971 Cell death during the development of the imaginal discs of *Calliphora erythrocephala*. Neth. J. Zool. **21:** 221–264.

Stronach, B., 2005 Dissecting JNK signaling, one KKKinase at a time. Dev. Dyn. **232:** 575–584.

Takatsu, Y., M. Nakamura, M. Stapleton, M. C. Danos, K. Matsumoto *et al.*, 2000 TAK1 participates in c-Jun N-terminal kinase signaling during Drosophila development. Mol. Cell. Biol. **20:** 3015–3026.

Vernooy, S. Y., J. Copeland, N. Ghaboosi, E. E. Griffin, S. J. Yoo *et al.*, 2000 Cell death regulation in Drosophila: conservation of mechanism and unique insights. J. Cell Biol. **150:** F69–F76.

Wang, S. L., C. J. Hawkins, S. J. Yoo, H. A. Muller and B. A. Hay, 1999 The Drosophila caspase inhibitor DIAP1 is essential for cell survival and is negatively regulated by HID. Cell **98:** 453–463.

White, K., E. Tahaoglu and H. Steller, 1996 Cell killing by the Drosophila gene reaper. Science **271:** 805–807.

Wu, J. W., A. E. Cocina, J. Chai, B. A. Hay and Y. Shi, 2001 Structural analysis of a functional DIAP1 fragment bound to grim and hid peptides. Mol. Cell **8:** 95–104.

Yan, N., J. W. Wu, J. Chai, W. Li and Y. Shi, 2004 Molecular mechanisms of DrICE inhibition by DIAP1 and removal of inhibition by Reaper, Hid and Grim. Nat. Struct. Mol. Biol. **11:** 420–428.

Yoo, S. J., J. R. Huh, I. Muro, H. Yu, L. Wang *et al.*, 2002 Hid, Rpr and Grim negatively regulate DIAP1 levels through distinct mechanisms. Nat. Cell Biol. **4:** 416–424.

Communicating editor: J. A. Birchler